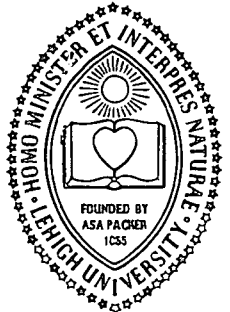


AT&T 17009 IFSM-72-13

N73-20912



LEHIGH UNIVERSITY

INSTITUTE OF
MECHANICAL
FRACTURE AND SOLID
MECHANICS

CASE FILE COPY

ALTERNATING METHOD APPLIED TO
EDGE AND SURFACE CRACK PROBLEMS

by
R. J. Hartranft
and
G. C. Sih

Technical Report NASA-TR-72-1

April 1972

NATIONAL AERONAUTICS AND SPACE ADMINISTRATION
LANGLEY RESEARCH CENTER
HAMPTON, VIRGINIA 23365

Page Intentionally Left Blank

ABSTRACT

The Schwarz-Neumann alternating method is employed to obtain stress intensity solutions to two crack problems of practical importance: (1) a semi-infinite elastic plate containing an edge crack which is subjected to concentrated normal and tangential forces, and (2) an elastic half-space containing a semicircular surface crack which is subjected to uniform opening pressure. The solution to the semicircular surface crack is seen to be a significant improvement over existing approximate solutions. Application of the alternating method to other crack problems of current interest is briefly discussed.

RECORDED
IN THE
CITY OF
DETROIT
MICHIGAN
ON THE
15TH DAY OF
JULY
BY
THE
DETROIT
POLICE
DEPARTMENT
AT THE
DETROIT
POLICE
STATION
IN THE
CITY OF
DETROIT
MICHIGAN

Page Intentionally Left Blank

NATIONAL AERONAUTICS AND SPACE ADMINISTRATION

Grant NGR-39-007-066

Technical Report No. 1

ALTERNATING METHOD
APPLIED TO
EDGE AND SURFACE CRACK PROBLEMS

by

R. J. Hartranft
Assistant Professor of Mechanics

and

G. C. Sih
Professor of Mechanics

Department of Mechanical Engineering and Mechanics
Lehigh University
Bethlehem, Pennsylvania

Approved for public release
April 1972
Distribution unlimited

Page Intentionally Left Blank

TABLE OF CONTENTS

	Page
LIST OF FIGURES	iii
NOTATION	iv
1. INTRODUCTION	1
2. EDGE CRACK PROBLEM	7
2.1 Infinite Plate with a Central Crack	11
2.2 Edge-Loaded Semi-Infinite Plate	19
2.3 Iterative Formulation of the Problem	20
2.4 Numerical Results and Green's Function	27
3. SURFACE CRACK PROBLEM	32
3.1 Penny-Shaped Crack in an Infinite Body	33
3.2 Surface Loads on Half Space	46
3.2(1) Nonsingular stress	46
3.2(2) Singular stress	49
3.3 Iterative Formulation	50
3.4 Numerical Treatment of Singularities	56
3.4(1) Half space	56
3.4(2) Penny-shaped crack - nonsingular load	58
3.4(3) Penny-shaped crack - singular load	61
3.5 Discussion of Numerical Results	64
4. FUTURE APPLICATIONS - SEMI-ELLIPTICAL CRACK	66
APPENDIX	70
REFERENCES	78
FIGURES	81

Page Intentionally Left Blank

List of Figures

<u>Figure</u>	<u>Title</u>
2.1	Edge-cracked plate
2.2	Cracked infinite plate
2.3	Edge-loaded half plane
2.4	Concentrated forces on an edge crack
2.5	Stress intensity factor correction for concentrated forces on an edge crack
3.1	Penny-shaped crack in infinite body
3.2	Local coordinates (ρ, ϕ) at crack front
3.3	Half space ($x \geq 0$) loaded on surface ($x=0$)
3.4	Auxiliary coordinates for singular solutions
3.5	Function for eq.(3.39) for singular normal stress on half-space
3.6	Half-penny surface crack
3.7	Grid on surface of half-space
3.8	Stress intensity factor for Figure 3.6
3.9	Successive iterations for stress intensity factor
3.10	Separate contributions to the stress intensity factor in first iteration
4.1	Semi-elliptical surface crack
A-1	Linearly loaded edge crack
A-2	Partially loaded edge crack
A-3	Correction factors for partially loaded edge crack
A-4	Penny-shaped crack in an infinite body under uniaxial tension and uniform shear
A-5	Concentrated forces on a penny-shaped crack
A-6	Penny-shaped crack in a cross-section of a beam under pure bending

Page Intentionally Left Blank

NOTATION

$\sigma_{xA}^{(n)}$, $\sigma_{yA}^{(n)}$, etc.	- n^{th} solution in sequence A
$\sigma_{xB}^{(n)}$, $\sigma_{yB}^{(n)}$, etc.	- n^{th} solution in sequence B
E, ν	- modulus of elasticity, Poisson's ratio
$J_m(x)$	- Bessel function of first kind of order m
$j_m(x)$	- spherical Bessel function of first kind of order m

Edge Crack

a	- length of edge crack, half length of crack in infinite medium
b	- distance from edge to concentrated force
$B(\alpha)$	- arbitrary function in solution of Section 2.1
c	- b/a
$f(b/a)$	- k_1, k_2 correction for concentrated forces
$F_0(y, z)$	- nonsingular stress on $x=0$ for uniform pressure on crack
$F_{mn}(y)$	- function involved in representation of $q(y, 0)$
k_1, k_2	- stress intensity factors in Mode I, II
$k_1^{(n)}, k_2^{(n)}$	- contribution of n^{th} iteration to k_1, k_2
$p^{(n)}(y), q^{(n)}(x)$	- normal stresses on planes $x=0, y=0$ in n^{th} iteration
P, Q	- concentrated forces on the crack
r	- distance from crack tip
$s^{(n)}(\xi), t^{(n)}(u)$	- dimensionless forms of $q^{(n)}(x), p^{(n)}(y)$

Page Intentionally Left Blank

$u = y/(a+y)$	- variable to reduce infinite range of integration to finite range
u_x, v_y	- displacement components
$v(x)$	$= \frac{E}{2(1-\nu^2)} v_y(x,0)$, displacement on $y=0$
$\sigma(x)$	- normal stress ($-\sigma_y(x,0)$) applied to crack
$\sigma_x, \sigma_y, \tau_{xy}$	- stress components
$\psi(t)$	- function introduced to solve for $v(x)$ and $B(\alpha)$

Surface Crack

a	- radius of penny-shaped crack, used to non-dimensionalize all lengths
A_{mn}	- coefficient of $r^n \cos 2(m-1)\theta$ in expansion of $p(r,\theta)$
b	- size of square in half space solution
C_{mn}	- coefficient of t^n in expansion of $g_{2m-2}(t)$
$D_m(\xi)$	- arbitrary functions in solution of Section 3.1
$F(\xi, \eta, \zeta)$	- Love's solution for normal stress on $z=0$ due to unit tension on a square of $x=0$ (half space)
$g_m(t)$	- functions introduced to solve for $w_m(r)$ and $D_m(\xi)$
I_k	- $I_0 = \pi/2$, $I_1 = 1$, $I_k = \frac{k-1}{k} I_{k-2}$
k_p	- stress intensity factor
$k(\theta)$	- dimensionless stress intensity factor, $k_p / (\frac{2}{\pi} p_0 \sqrt{a})$
$k^{(n)}(\theta)$	$= \frac{4\nu}{\pi} k^{(n-1)}(\frac{\pi}{2}) k_S(\theta) + k_N^{(n)}(\theta)$, contribution of n^{th} iteration to $k(\theta)$

Page Intentionally Left Blank

$k_N^{(n)}(\theta)$	- $k(\theta)$ produced by $\sigma_z = p_0 t_N^{(n)}(x,y)$ on crack
$k_S(\theta)$	- $k(\theta)$ produced by singular stress (Section 3.4(3)) on crack
$K_m(r)$	- Fourier coefficients of $p(r,\theta)$
p_c	- dimensionless pressure at center of crack
p_0	- uniform pressure on crack, used to non-dimensionalize boundary stresses
$p(r,\theta)$	- dimensionless variable pressure on crack
$q^{(n)}(y,z)$	= $\frac{4v}{\pi} k^{(n-1)}(\frac{\pi}{2}) q_S(y,z) + q_N^{(n)}(y,z)$, dimensionless, nonsingular part of σ_x on $x=0$ in n^{th} iteration
$q_N^{(n)}(y,z)$	- nonsingular part of σ_x on $x=0$ produced by $\sigma_z = t_N^{(n)}(x,y)$ on crack
$q_S(y,z)$	- nonsingular part of σ_x on $x=0$ produced by singular stress (Section 3.4(3)) on crack
r, θ, z	- dimensionless cylindrical coordinates
R_1, ψ_1, R_2, ψ_2	- dimensionless coordinates in plane of crack
$S(\psi)$	- function giving singular σ_z on crack due to singular part of σ_x on $x=0$
$t^{(n)}(x,y)$	= $\frac{4v}{\pi} k^{(n-2)}(\frac{\pi}{2}) t_S(x,y) + t_N^{(n)}(x,y)$, dimensionless, nonsingular stress on crack in n^{th} iteration
$t_N^{(n)}(x,y)$	- stress on crack produced by $\sigma_x = q_N^{(n-1)}(y,z)$ on $x=0$

Page Intentionally Left Blank

$t_S(x,y)$	- stress on crack produced by $\sigma_x = q_S(y,z)$ on $x=0$
u_r, v_θ, w_z	- displacement components in cylindrical coordinates
$w_m(r)$	- displacement-like functions related to $w_z(r,\theta,0)$
ρ, ϕ	- dimensionless local polar coordinates at the crack front
$\rho_1, \phi_1, \rho_2, \phi_2$	- dimensionless coordinates on the surface
$\sigma_r, \sigma_\theta, \sigma_z$	- stress components in cylindrical coordinates
$\tau_{\theta z}, \tau_{rz}, \tau_{r\theta}$	
μ	$= \frac{E}{2(1+\nu)}$, shear modulus

Page Intentionally Left Blank

ALTERNATING METHOD APPLIED TO EDGE AND
SURFACE CRACK PROBLEMS

by

R. J. Hartranft and G. C. Sih
Lehigh University

1. INTRODUCTION

Over the past decade, numerous analytical solutions of crack problems have appeared in the open literature [1]*. A great number of these solutions are concerned with idealized crack geometries in plane or axisymmetric elasticity. However, only a few problems involving the interaction of cracks with neighboring boundaries have been solved satisfactorily. In situations where the crack intersects a free edge or surface, the method of solution becomes much more difficult and requires special attention. The advent of computers has no doubt facilitated the numerical computation of stress distributions around cracks. Without them, many of the tedious calculations would not be attempted. The alternating method is one which intimately combines analytical results with the numerical calculations.

One of the requisites for solving any crack problem is to handle the stress singularities at the crack tips properly. This involves first of all a knowledge of the correct behavior of the stress singularity, which is a task normally accomplished

* Numbers in square brackets designate one of the References at the end of the Chapter.

by analytical means. Next, it is essential to preserve this singular behavior of the solution in the problem either by isolating it away from numerical computations or by treating it numerically with the utmost care. Generally speaking, the error committed near a singular point such as a crack tip or border will not be confined locally but will cause errors elsewhere as well. The same applies to corners or points in the elastic solid where high stress gradients are present. This point will be demonstrated in the present work on the surface crack problem in three dimensions.

What follows is a treatment of the alternating method as applied to solve edge crack problems in two-dimensions and surface crack problems in three-dimensions. Although the surface crack solution is not complete, it serves as a good example for illustrating the complexities and understanding required to treat problems of this type. The mechanics of the alternating method is in fact rather rudimentary. It is described in the work of Kantorovich and Krylov [2] who obtained the solutions to potential problems by using successive, iterative superposition of sequences of solutions. Their illustration involves two sequences of solutions, each sequence applying to a particular geometry. By the alternating superposition of the sequences, the solution for the region common to both geometries may be found. The method is called the Schwarz-Newmann Alternating Technique in their book. In this work it will be referred to as the alternating method, and it

will be applied to solve elastic crack problems.

As an example of the alternating method, consider a simple problem with no singularities. Suppose the stresses in the quarter plane $x \geq 0$, $y \geq 0$ are to be found for the boundary conditions

$$\tau_{xy}(0,y) = 0 \quad \tau_{xy}(x,0) = 0$$

$$\sigma_x(0,y) = 0 \quad \sigma_y(x,0) = \sigma(x)$$

One sequence of solutions, Sequence A, leads from the stress $\sigma_{yA}(x,0) = q(x)$ on the half plane $y \geq 0$ to the stress $\sigma_{xA}(0,y) = p(y)$ in particular and to all other stresses in the quarter plane considered. The second, Sequence B, for $x \geq 0$ leads from $\sigma_{xB}(0,y) = p(y)$ to a solution yielding $\sigma_{yB}(x,0) = q(x)$. The sequences, A and B, may be formed to yield the solution for the quarter plane common to both half planes.

From A, let $q^{(0)}(x) = \sigma(x)$, $x > 0$ and $q^{(0)}(x) = \sigma(-x)$, $x < 0$.

For the first solution in sequence A,

$$\sigma_{yA}^{(1)}(x,0) = q^{(0)}(x) \text{ yields } \sigma_{xA}^{(1)}(0,y) = p^{(1)}(y), \text{ say.}$$

For the first solution in sequence B,

$$\sigma_{xB}^{(1)}(0,y) = -p^{(1)}(y) \text{ yields } \sigma_{yB}^{(1)}(x,0) = -q^{(1)}(x), \text{ say.}$$

Next in sequence A,

$$\sigma_{yA}^{(2)}(x,0) = q^{(1)}(x) \text{ yields } \sigma_{xA}^{(2)}(0,y) = p^{(2)}(y), \text{ say}$$

and then in sequence B,

$$\sigma_{xB}^{(2)}(0,y) = -p^{(2)}(y) \text{ yields } \sigma_{yB}^{(2)}(x,0) = -q^{(2)}(x), \text{ say.}$$

The sequences continue alternating this way. Both sequences apply to the quarter plane, and by superposition, the boundary values on the quarter plane are

$$\sigma_y(x,0) = \sigma_{yA}^{(1)}(x,0) + \sigma_{yB}^{(1)}(x,0) + \sigma_{yA}^{(2)}(x,0) + \sigma_{yB}^{(2)}(x,0) + \dots$$

$$\sigma_x(0,y) = \sigma_{xA}^{(1)}(0,y) + \sigma_{xB}^{(1)}(0,y) + \sigma_{xA}^{(2)}(0,y) + \sigma_{xB}^{(2)}(0,y) + \dots$$

or

$$\sigma_y(x,0) = q^{(0)}(x) - q^{(1)}(x) + q^{(1)}(x) - q^{(2)}(x) + \dots$$

$$\sigma_x(0,y) = p^{(1)}(y) - p^{(1)}(y) + p^{(2)}(y) - p^{(2)}(y) + \dots$$

Therefore, after superposing the first n terms of each sequence, the boundary values are

$$\sigma_y(x,0) = \sigma(x) - q^{(n)}(x)$$

$$\sigma_x(0,y) = 0$$

Additional solutions from the sequences are superposed until the residual stress, $q^{(n)}(x)$, on the x-axis is negligible

compared to the applied stress $\sigma(x)$.

A different form of the alternating method was applied to the problem of an edge crack in a semi-infinite region by Irwin [3], who essentially used only the first few solutions of each sequence to estimate the stress intensity factor. Lachenbruch [4] included additional terms from each sequence to obtain a better estimate. Further study of the alternating method applied to this problem will be carried out in detail in Section 2. One of the two sequences of solutions involved there is for an infinite region containing a finite straight-crack subjected to arbitrary normal stresses on its faces. The solution is written in integral form and may be evaluated for any given loads. In this case, the analytical result gives the singularity separately, and no additional special numerical treatment is required.

Recently, application of the alternating method to finite width strips cracked on one edge has been formulated by Brož [5]. The method of Section 2 could be extended to this case by using three sequences of solutions. Reference to such extensions will be made later on. However, Brož considers more complicated analytical problems involving only two sequences. One sequence considers a row of collinear equally spaced cracks of equal length, each loaded by the same arbitrary normal stresses on its faces. He gives the formulas for the stresses at the locations of the edges of the strip in terms of integrals which may be numerically evaluated.

The other sequence gives a similar expression for the stress produced at the location of the crack in an uncracked strip loaded arbitrarily on its edges. He has included very few numerical results in [5], but a computer program for obtaining additional results could be easily written.

In a similar fashion, three-dimensional problems may also be solved by the alternating method. Smith et al. [6,7,8] have published a series of papers containing numerical results for the effect of interaction of cracks with free surfaces. One of the geometries considered [6] was a surface crack perpendicular to the surface of a half space. The crack is in the shape of half of a flat circular disk with the diameter on the surface. The other problems involved cases where the crack is a larger or smaller portion of the circular disk whose diameter parallel to the surface lies either above or below the surface. In [7] the crack intersects the free surface, and in [8] it is completely embedded in the half space. A generalization of [8] was later made by Shah and Kobayashi [9] in which the embedded crack is elliptical in shape with the minor axis perpendicular to the surface.

As in the plane problems, one sequence of solutions for the three-dimensional problems above is chosen to be an infinite body containing a crack. For the penny-shaped crack a fairly convenient solution is known for pressure on the crack of the form $r^n \cos n\theta$ where r and θ are the usual polar coordinates. A less convenient solution for the elliptical crack is known for polynomial variations of the stress on

the crack. But these solutions account only partially for the effect of the stress singularity. The other sequence used for the three-dimensional problems is made up of solutions of arbitrarily loaded half spaces. It may be seen in Section 3 that the stress applied to the half space must be singular. The previous solutions do not satisfactorily treat this effect, which is shown in Section 3.5 to drastically alter the numerical results. The singularity on the surface of the half space may be taken care of analytically, and then one is faced with an additional singularity in the other sequence. That is, the stress applied to the crack is singular at two points of the crack front. No analytical way of handling this singularity could be found at present, but special precaution was taken numerically.

2. EDGE CRACK PROBLEM

The determination of stress intensity factors for bodies containing cracks extending inward from a free edge has attained importance because such cracks are frequently found in structural members. The analytical model is usually based on the theory of elasticity in plane strain or generalized plane stress. The case of a crack perpendicular to the edge of a semi-infinite material (Figure 2.1) will be considered.

Figure 2.1

Irwin [3,10] estimated the stress intensity factor, k_1 , for the case of uniform pressure on the edge crack (or uniform tension at infinity perpendicular to the crack) and obtained a value of k_1 ten percent higher than that for an infinite plate with a crack of twice the length. He used two problems whose solutions are given in Sections 2.1 and 2.2. The infinite plate with an arbitrarily pressurized crack is considered first. Then the half plate subjected to arbitrary normal stresses is superposed on the infinite cracked plate. Irwin used the superposition to obtain two simultaneous integral equations (see Section 2.3) in two unknown functions and solved them by an iterative method which is equivalent to the alternating method presented here.

Later, Bueckner [11] reconsidered the problem and obtained a more accurate correction (13%)*. By superposing the two problems described above, he obtained a singular integral equation for the deformed shape of the crack. The equation permitted straightforward integration for obtaining the pressure required to produce certain prescribed deformed shapes. A number of different deformed shapes and associated pressure distributions were obtained. A linear combination of these pressures was fitted to the actual uniform pressure by collocation (equating the actual pressure to the linear

* Winne and Wundt [12] overlooked the correction of Bueckner when they used some of his other results on cracks in finite width strips (also contained in [11]). The review of Paris and Sih [1] points out the error in [12].

combination at a number of points equal to the number of undetermined coefficients). Thus the deformed shape of the crack was determined as a known linear combination of the prescribed shapes. And the stress intensity factor followed immediately (as from equation (2.16) below).

Koiter [13], in his analysis of the same problem, gave a refined value of the stress intensity factor involving a correction of 12.15%. The computation of a definite integral was done numerically with such precision that the factor above is in error by no more than one unit in the last digit. The definite integral results from the application [14] of Mellin transforms [15] to the quarter plane problem to which the one under consideration reduces by symmetry. The transform leads to an equation of the WIENER-HOPF type which is then solved.

Table I: k_1 values for uniform tension in Figure 2.1

Source	$k_1 / \sigma\sqrt{a}$
Irwin [3,10]	1.1
Bueckner [11]	1.13
Koiter [13,14]	1.1215
Wigglesworth [16]	1.122
Lachenbruch [4]	1.1
Stallybrass [18]	1.1215
Sneddon [19]	1.1215
Appendix	1.1215*

* obtained by using equation (2.50).

A more general study of the problem using the alternating method, was made by Lachenbruch [4], who considered variable as well as uniform loads on the crack.

There have been other solutions [16,17,18] of the problem using the same technique as in [13,14]. The latest by Stallybrass [18] obtains the stress intensity factors for stress on the crack varying as a power of distance from the edge. He gives numerical results for integer powers, 0, 1, 2, ... 10, which could be combined if the stress on the crack is a polynomial function of that distance. Sneddon [19] also used the quarter plane formulation, but his technique of solving the problem (similar to the method of Section 2.1) leads to a Fredholm integral equation of the second kind. Two approximate methods of solving the integral equation are compared for the case of uniform stress on the crack, and both give very good accuracy.

Sections 2.1 and 2.2 which follow contain the solutions of the two problems used in the alternating method. The alternating method is presented in detail in Section 2.3 for the case of concentrated forces acting on the crack. The numerical results of Section 2.4 are used to develop an integral expression for the stress intensity factor for arbitrary loads on the crack. The integral is evaluated for several examples which are contained in the Appendix. One of the examples is the problem of uniform pressure on the crack which has been considered by many others. A comparison of this

result with those obtained by the various other investigators can be found in Table I.

2.1 Infinite Plate With a Central Crack

The method of integral transforms [15] may be used to obtain a solution of the equations of elasticity general enough to satisfy the boundary conditions of this problem. Formulas from Chapter 9 of [15] for the special case of symmetry about the x- and y-axes may be written in integral form. For the present work, it is sufficient to note that the expressions satisfy all of the equations of elasticity by direct substitution. For the case of plane strain the displacements u_x and v_y in the x- and y-directions, respectively, are given by

$$\frac{E}{1+\nu} u_x = - \int_0^{\infty} [(1-2\nu)-\alpha y] B(\alpha) e^{-\alpha y} \sin \alpha x d\alpha \quad (2.1)$$

$$\frac{E}{1+\nu} v_y = \int_0^{\infty} [2(1-\nu)+\alpha y] B(\alpha) e^{-\alpha y} \cos \alpha x d\alpha$$

where E and ν are the modulus of elasticity and Poisson's ratio. $B(\alpha)$ is a function which will be determined by the boundary conditions. The stresses associated with the displacement field of equations (2.1) are

$$\sigma_x = - \int_0^{\infty} (1-\alpha y) \alpha B(\alpha) e^{-\alpha y} \cos \alpha x d\alpha \quad (2.2)$$

$$\sigma_y = - \int_0^{\infty} (1+\alpha y) \alpha B(\alpha) e^{-\alpha y} \cos \alpha x d\alpha$$

$$\tau_{xy} = -y \int_0^{\infty} \alpha^2 B(\alpha) e^{-\alpha y} \sin \alpha x d\alpha$$

The solution given by equations (2.1) and (2.2) may also be used for generalized plane stress if E is replaced by $(1+2v)E/(1+v)^2$ and v by $v/(1+v)$. Equations (2.1) and (2.2) should be applied only for $y \geq 0$. For negative y , the conditions of symmetry about the x -axis should be used. The crack problem of this Section is restricted to the case of loading by normal stresses on the crack which are symmetric about the y -axis. With this restriction, the problem has the symmetry required for application of equations (2.1) and (2.2). It may be noticed that the last of equations (2.2) satisfies the boundary condition $\tau_{xy}(x,0) = 0$ on the crack and the x -axis of symmetry outside of the crack.

Figure 2.2

The boundary conditions which determine the value of $B(\alpha)$ are

$$\sigma_y(x,0) = -q(x), \quad |x| < a \quad v_y(x,0) = 0, \quad |x| > a \quad (2.3)$$

where the first of equations (2.3) comes from the imposed pressure, $q(x)$, on the crack. The second of equations (2.3) results from symmetry about the x -axis.

The boundary conditions (2.3) require these special results from eqs.(2.1) and (2.2):

$$\frac{E}{1+\nu} v_y(x,0) = 2(1-\nu) \int_0^{\infty} B(\alpha) \cos \alpha x d\alpha$$

$$\sigma_y(x,0) = - \int_0^{\infty} \alpha B(\alpha) \cos \alpha x d\alpha \quad (2.4)$$

$$\text{Let } v(x) = \frac{E}{2(1-\nu^2)} v_y(x,0) = \int_0^{\infty} B(\alpha) \cos \alpha x d\alpha \quad (2.5)$$

The Fourier inversion [15] of equation (2.5) gives

$$B(\alpha) = \frac{2}{\pi} \int_0^{\infty} v(x) \cos \alpha x dx$$

But by the second of equations (2.3), $v(x) = 0$ for $x > a$.

Therefore, $B(\alpha)$ becomes

$$B(\alpha) = \frac{2}{\pi} \int_0^a v(x) \cos \alpha x dx \quad (2.6)$$

Now, since $v(x)$ is a displacement, the representation

$$v(x) = \int_x^a \frac{\psi(t) t dt}{\sqrt{t^2 - x^2}}, \quad 0 < x < a \quad (2.7)$$

may be used. Integration of equation (2.7) by parts shows the correct crack tip opening shape. If equation (2.7) is substituted into equation (2.6),

$$\begin{aligned}
 B(\alpha) &= \frac{2}{\pi} \int_0^a \cos \alpha x dx \int_x^a \frac{\psi(t) t dt}{\sqrt{t^2 - x^2}} \\
 &= \frac{2}{\pi} \int_0^a \psi(t) t dt \int_0^t \frac{\cos \alpha x}{\sqrt{t^2 - x^2}} dx \\
 &= \int_0^a \psi(t) J_0(\alpha t) t dt
 \end{aligned} \tag{2.8}^*$$

The first of equations (2.3) and the second of (2.4) give the equation

$$\int_0^\infty \alpha B(\alpha) \cos \alpha x d\alpha = q(x), \quad 0 < x < a \tag{2.9}$$

Integrating equation (2.9),

$$\int_0^\infty B(\alpha) \sin \alpha x d\alpha = \int_0^x q(\xi) d\xi, \quad 0 < x < a \tag{2.10}$$

If equation (2.8) is substituted into equation (2.10) an integral equation for $\psi(t)$ results.

$$\begin{aligned}
 \int_0^\infty \sin \alpha x d\alpha \int_0^a \psi(t) J_0(\alpha t) t dt &= \int_0^x q(\xi) d\xi, \quad 0 < x < a \\
 \text{or } \int_0^a \psi(t) t dt \int_0^\infty J_0(\alpha t) \sin \alpha x d\alpha &= \int_0^x q(\xi) d\xi, \quad 0 < x < a
 \end{aligned} \tag{2.11}$$

* The formula for $J_0(x)$, the Bessel function of order zero, on page 27 of [20] is used in the last step.

But*

$$\int_0^\infty J_0(at) \sin \alpha x d\alpha = \begin{cases} 0 & t > x \\ \frac{1}{\sqrt{x^2 - t^2}} & t < x \end{cases}$$

Therefore, equation (2.11) reduces to

$$\int_0^x \frac{\psi(t)tdt}{\sqrt{x^2 - t^2}} = \int_0^x q(\xi)d\xi, \quad 0 < x < a \quad (2.12)$$

Equation (2.12) may be solved as a special case of Abel's integral equation**

$$\int_0^x \frac{\phi(t)dt}{\sqrt{x^2 - t^2}} = h(x), \quad 0 < x < a \quad (2.13)$$

which has the solution

$$\phi(t) = \frac{2}{\pi} \left\{ t \int_0^t \frac{h'(x)dx}{\sqrt{t^2 - x^2}} + h(0) \right\}, \quad 0 < t < a \quad (2.14)$$

Therefore, the solution of equation (2.12) is

$$\psi(t) = \frac{2}{\pi} \int_0^t \frac{q(x)dx}{\sqrt{t^2 - x^2}}, \quad 0 < t < a \quad (2.15)$$

It is known that the opening displacement of the crack tip is given by (see equations (3.15) of [21])

* First formula on page 37 of [20].

** This form may be obtained from that on page 141 of [20] by a change of variables.

$$v_y(x,0) = \frac{2(1-\nu^2)}{E} k_1 \sqrt{2r} + O(r) \quad (2.16)$$

for plane strain. In this result, $r = a-x$, and k_1 is the Mode I stress intensity factor. From equation (2.5)

$$v_y(x,0) = \frac{2(1-\nu^2)}{E} v(x) \quad (2.17)$$

and from equation (2.7) for $x = a-r$,

$$v(x) = \int_{a-r}^a \frac{\psi(t) t dt}{\sqrt{t^2 - (a-r)^2}} = \int_0^r \frac{a-p}{\sqrt{r-p}} \frac{\psi(a-p) dp}{\sqrt{2a-r-p}} \quad (2.18)$$

In equation (2.18), when r is small, r and p may be neglected in comparison with a , and then

$$\begin{aligned} v(x) &= \frac{a\psi(a)}{\sqrt{2a}} \int_0^r \frac{dp}{\sqrt{r-p}} + O(r) \\ &= \sqrt{2r} \sqrt{a} \psi(a) + O(r) \end{aligned} \quad (2.19)$$

Thus, by comparing equations (2.16), (2.17), (2.19), the stress intensity factor

$$k_1 = \sqrt{a} \psi(a)$$

is obtained. Hence, utilizing equation (2.15),

$$k_1 = \frac{2}{\pi} \sqrt{a} \int_0^a \frac{q(x) dx}{\sqrt{a^2 - x^2}} \quad (2.20)$$

It is also necessary to evaluate the normal stress on the y-axis which, from equations (2.2), is

$$\sigma_x(0,y) = - \int_0^\infty (1-\alpha y) \alpha B(\alpha) e^{-\alpha y} d\alpha \quad (2.21)$$

From equations (2.8) and (2.15)

$$\begin{aligned} B(\alpha) &= \frac{2}{\pi} \int_0^a J_0(\alpha t) t dt \int_0^t \frac{q(x) dx}{\sqrt{t^2 - x^2}} \\ &= \frac{2}{\pi} \int_0^a q(x) dx \int_x^a \frac{J_0(\alpha t)}{\sqrt{t^2 - x^2}} t dt \end{aligned}$$

Therefore, interchanging the order of integration in equation (2.21),

$$\sigma_x(0,y) = \frac{2}{\pi} \int_0^a f(x,y) q(x) dx \quad (2.22)$$

$$\text{where } f(x,y) = \int_x^a g(y,t) \frac{tdt}{\sqrt{t^2 - x^2}} \quad (2.23)$$

$$\text{where } g(y,t) = - \int_0^\infty (1-\alpha y) \alpha J_0(\alpha t) e^{-\alpha y} d\alpha$$

The evaluation of $g(y,t)$ leads directly to

$$g(y,t) = y \frac{y^2 - 2t^2}{(t^2 + y^2)^{5/2}} \quad (2.24)$$

The integration of equation (2.23) may be accomplished with $g(y,t)$ given by equation (2.24). The result is

$$f(x,y) = \frac{y}{x^2+y^2} \sqrt{\frac{a^2-x^2}{a^2+y^2}} \left[\frac{2y^2}{x^2+y^2} - \frac{2a^2+y^2}{a^2+y^2} \right] \quad (2.25)$$

Finally, substituting equation (2.25) into (2.22), the integral

$$p(y) = \frac{2}{\pi} \frac{y}{\sqrt{a^2+y^2}} \int_0^a q(x) \frac{\sqrt{a^2-x^2}}{x^2+y^2} \left[\frac{2y^2}{x^2+y^2} - \frac{2a^2+y^2}{a^2+y^2} \right] dx \quad (2.26)$$

for the desired stress,

$$\sigma_x(0,y) = p(y) \quad (2.27)$$

is obtained.

The above results apply also to the case of shear loading on the crack. In fact if the stress on the crack is

$$\tau_{xy}(x,0) = -q(x), \quad |x| < a$$

where $q(x) = q(-x)$, then the Mode II stress intensity factor is

$$k_2 = \frac{2}{\pi} \sqrt{a} \int_0^a \frac{q(x)dx}{\sqrt{a^2-x^2}} \quad (2.28)$$

and

$$\tau_{xy}(0,y) = p(y)$$

where $p(y)$ is given by equation (2.26).

2.2 Edge-Loaded Semi-Infinite Plate

The solution given by equations (2.1) and (2.2) applies to the case in which a half plane, $y \geq 0$ (Figure 2.3) is subjected to normal stresses

$$\sigma_y(x, 0) = p(x) \quad (2.29)$$

symmetric about the y -axis. It is found from the second of equations (2.2) and the Fourier inversion theorem that

$$\alpha B(\alpha) = -\frac{2}{\pi} \int_0^{\infty} p(x) \cos \alpha x dx \quad (2.30)$$

Figure 2.3

The first of equations (2.2) and equation (2.30) combine to give

$$\begin{aligned} \sigma_x(0, y) &= \frac{2}{\pi} \int_{-0}^{\infty} (1-\alpha y) \alpha e^{-\alpha y} d\alpha \int_0^{\infty} p(x) \cos \alpha x dx \\ &= \frac{2}{\pi} \int_0^{\infty} p(x) dx \int_0^{\infty} (1-\alpha y) \alpha e^{-\alpha y} \cos \alpha x d\alpha \\ &= \frac{4}{\pi} y \int_0^{\infty} \frac{x^2 p(x) dx}{(x^2 + y^2)^2} \end{aligned} \quad (2.31)$$

A change of coordinates gives us that for a half plane, $x \geq 0$, subjected to tension on the edge,

$$\sigma_x(0, y) = p(y) \quad (2.32)$$

the desired stress is

$$\sigma_y(x,0) = \frac{4}{\pi} x \int_0^{\infty} \frac{y^2 p(y) dy}{(x^2 + y^2)^2} \quad (2.33)$$

For convenience in the numerical work, introduce the new variable,

$$u = \frac{y}{a+y}$$

and the function,

$$t(u) = u^2 p(y) = u^2 p\left(\frac{au}{1-u}\right)$$

In terms of these quantities,

$$\sigma_y(x,0) = \frac{4}{\pi} \frac{x}{a} \int_0^1 \frac{t(u) du}{[x^2(1-u)^2/a^2+u^2]^a} \quad (2.34)$$

Again, the case of shear loading

$$\tau_{xy}(0,y) = p(y) \quad (2.35)$$

on a half plane has a similar solution yielding

$$\tau_{xy}(x,0) = \frac{4}{\pi} x \int_0^{\infty} \frac{y^2 p(y) dy}{(x^2 + y^2)^2} \quad (2.36)$$

2.3 Iterative Formulation of the Problem

The iterative approach may be thought about in two ways which are essentially equivalent. One way used by Irwin [3], involves the superposition of the preceding two

solutions. The boundary conditions of the edge-cracked plate problem result in a pair of integral equations:

$$q(x) - \frac{4}{\pi} x \int_0^{\infty} \frac{y^2 p(y) dy}{(x^2 + y^2)^2} = \sigma(x), \quad 0 \leq x \leq a$$

and

$$p(y) + \frac{2}{\pi} \frac{y}{\sqrt{a^2 + y^2}} \int_0^a \frac{q(x) \sqrt{a^2 - x^2}}{x^2 + y^2} \left[\frac{2y^2}{x^2 + y^2} - \frac{2a^2 + y^2}{a^2 + y^2} \right] dx = 0, \\ 0 \leq y < \infty$$

where $\sigma(x)$ is the stress applied to the edge crack. These equations may be solved by iteration by assuming some form for $q(x)$, say $q(x) = \sigma(x)$, and using this assumed form in the second equation to solve for $p(y)$. This value of $p(y)$ is then used in the first equation to obtain a corrected value of $q(x)$. Then a corrected value of $p(y)$ is found, and the procedure is continued until there is no significant change in $p(y)$ or $q(x)$. The last value of $q(x)$ gives the stress intensity factor according to equation (2.20).

A more satisfactory way, from a physical and computational point of view, of interpreting the iterative approach involves the alternating superposition of the previously developed solutions. Consider the details of the case,

$$\sigma(x) = P\delta(x-b), \quad 0 < b < a$$

where $\delta(x)$ is the Dirac Delta generalized function. The above expression represents a line force, P (force per unit

length in the z-direction), acting a distance b from the free edge. (Figure 2.4).

Figure 2.4

Let us refer to the infinite plate containing the crack as Problem A, and to the edge-loaded semi-infinite plate as Problem B. Subscripts of A or B will denote the problem with which the subscripted stress is associated. Then the iterations consist of superimposing Problem A and Problem B. The procedure begins with Problem A.

In Problem A, let the stress on the crack be

$$\sigma_{yA}^{(0)}(x,0) = -q^{(0)}(x) = -\sigma(x) = -P\delta(x-b), \quad x>0 \quad (2.37)$$

and require it to be even in x . That is, the crack is opened by four symmetrically located concentrated forces. The present simple form of $\sigma(x)$ allows

$$k_1^{(0)} = \frac{2}{\pi} \frac{P\sqrt{a}}{\sqrt{a^2-b^2}}$$

and $\sigma_{xA}^{(0)}(0,y) = p^{(0)}(y)$

$$\text{where } p^{(0)}(y) = \frac{2P}{\pi} \frac{\sqrt{a^2-b^2}}{\sqrt{a^2+y^2}} \frac{y}{b^2+y^2} \left[\frac{2y^2}{b^2+y^2} - \frac{2a^2+y^2}{a^2+y^2} \right] \quad (2.39)$$

to be evaluated in closed form from equations (2.20) and (2.26). In the case of more complicated loading $k_1^{(0)}$ and $p^{(0)}(y)$ could

be evaluated by numerical integration as in the succeeding iterations. The second part of the zeroth integration involves Problem B.

In Problem B, let the normal stress on the edge be

$$\sigma_{xB}^{(0)}(0,y) = -p^{(0)}(y)$$

This load gives the stress according to equation (2.33) as

$$\sigma_{yB}^{(0)}(x,0) = q^{(1)}(x)$$

where $q^{(1)}(x) = -\frac{4}{\pi} x \int_0^{\infty} \frac{y^2 p^{(0)}(y) dy}{(x^2 + y^2)^2}$ (2.40)

The superposition of these two problems gives a stress state which satisfies all of the boundary conditions of the edge-cracked plate except that the stress on the crack is

$$\sigma_y(x,0) = -\sigma(x) + q^{(1)}(x)$$

If $q^{(1)}(x)$ is not negligible compared to $\sigma(x)$, further iterations are required.

The first part of the first iteration requires the solution of Problem A for

$$\sigma_{yA}^{(1)}(x,0) = -q^{(1)}(x)$$

This leads to an additional contribution to the stress intensity

factor of

$$k_1^{(1)} = \frac{2}{\pi} \sqrt{a} \int_0^a \frac{q^{(1)}(x) dx}{\sqrt{a^2 - x^2}}$$

and a stress on $x = 0$ of

$$\sigma_{xA}^{(1)}(0, y) = p^{(1)}(y)$$

where

$$p^{(1)}(y) = \frac{2}{\pi} \frac{y}{\sqrt{a^2 + y^2}} \int_0^a \frac{q^{(1)}(x) \sqrt{a^2 - x^2}}{x^2 + y^2} \left[\frac{2y^2}{x^2 + y^2} - \frac{2a^2 + y^2}{a^2 + y^2} \right] dx \quad (2.41)$$

An application of Problem B for a load of

$$\sigma_{xB}^{(1)}(0, y) = -p^{(1)}(y)$$

gives $\sigma_{yB}^{(1)}(x, 0) = q^{(2)}(y)$

where $q^{(2)}(y) = -\frac{4}{\pi} x \int_0^\infty \frac{y^2 p^{(1)}(y) dy}{(x^2 + y^2)^2}$

The superposition of these two parts of the first iteration gives the solution of the edge cracked plate with load on the crack,

$$\sigma_y^{(1)}(x, 0) = -q^{(1)}(x) + q^{(2)}(x)$$

After superposing the zeroth and first interations, the stress on the crack is

$$\sigma_y(x,0) = -\sigma(x) + q^{(2)}(x)$$

and the stress intensity factor is

$$k_1 = \frac{2}{\pi} \frac{P\sqrt{a}}{\sqrt{a^2-b^2}} + \frac{2}{\pi} \sqrt{a} \int_0^a \frac{q^{(1)}(x)dx}{\sqrt{a^2-x^2}}$$

The second iteration has the stresses

$$\sigma_{yA}^{(2)}(x,0) = -q^{(2)}(x) \quad \sigma_{xA}^{(2)}(0,y) = p^{(2)}(y)$$

$$\sigma_{xB}^{(2)}(0,y) = -p^{(2)}(y) \quad \sigma_{yB}^{(2)}(x,0) = q^{(3)}(x)$$

and the stress intensity factor associated with $q^{(2)}(x)$. The functions $p^{(2)}(y)$ and $q^{(3)}(x)$ are given by formulas similar to equations (2.40) and (2.41). After superposing this interation on the others, we have the edge-cracked plate subjected to stress

$$\sigma_y(x,0) = -\sigma(x) + q^{(3)}(x)$$

on the crack. For this load the stress intensity factor is

$$k_1 = \frac{2}{\pi} \sqrt{a} \left\{ \frac{P}{\sqrt{a^2-b^2}} + \int_0^a [q^{(1)}(x) + q^{(2)}(x)] \frac{dx}{\sqrt{a^2-x^2}} \right\}$$

The pattern of the iterations should be clear now.

For the computations, introduce the dimensionless variables

$$\xi = x/a \quad u = y/(a+y) \quad c = b/a$$

and the functions

$$s^{(n)}(\xi) = \frac{1}{p} \sqrt{a^2 - b^2} q^{(n)}(a\xi)$$

$$t^{(n)}(u) = \frac{u^2}{p} \sqrt{a^2 - b^2} p^{(n)}\left(\frac{au}{1-u}\right)$$

Then the iteration is from $t^{(0)}(u)$ to $s^{(1)}(\xi)$ to $t^{(1)}(u)$, etc.
where

$$t^{(0)}(u) = \frac{2}{\pi} \frac{1-c^2}{c^2(1-u)^2+u^2} \frac{u^3(1-u)^2}{\sqrt{(1-u)^2+u^2}} \left[\frac{2u^2}{c^2(1-u)^2+u^2} - \frac{2(1-u)^2+u^2}{(1-u)^2+u^2} \right] \quad (2.42)$$

$$s^{(n)}(\xi) = -\frac{4}{\pi} \xi \int_0^1 \frac{t^{(n-1)}(u) du}{[\xi^2(1-u)^2+u^2]^2}, \quad n \geq 1 \quad (2.43)$$

$$t^{(n)}(u) = \frac{2}{\pi} \frac{u^3(1-u)^2}{\sqrt{(1-u)^2+u^2}} \int_0^1 \frac{s^{(n)}(\xi) \sqrt{1-\xi^2}}{\xi^2(1-u)^2+u^2} \left[\frac{2u^2}{\xi^2(1-u)^2+u^2} - \frac{2(1-u)^2+u^2}{(1-u)^2+u^2} \right] d\xi, \quad n \geq 1 \quad (2.44)$$

In terms of

$$s(\xi) = s^{(1)}(\xi) + s^{(2)}(\xi) + \dots$$

the stress intensity factor is given by

$$k_1 = \frac{2}{\pi} \frac{P\sqrt{a}}{\sqrt{a^2 - b^2}} [1 + f(\frac{b}{a})] \quad (2.45)$$

where

$$f(c) = \int_0^1 \frac{s(\xi)d\xi}{\sqrt{1-\xi^2}}$$

The dependence of $f(c)$ on c comes from $t^{(0)}(u)$.

The stress intensity factor for the edge-cracked plate subjected to shear forces (Figure 2.4) is given in terms of the same function $f(c)$ above as

$$k_2 = \frac{2}{\pi} \frac{Q\sqrt{a}}{\sqrt{a^2 - b^2}} [1 + f(\frac{b}{a})] \quad (2.46)$$

2.4 Numerical Results and Green's Function

The numerical iteration of equations (2.42-44) is straightforward except when the concentrated forces are very near the edge of the plate. For $b/a \geq .2$ the integrals were evaluated using Simpson's rule with 250 subdivisions, and five iterations were used. Tests using more subdivisions and iterations showed that the accuracy of the results is about one percent. As b/a was decreased, more subdivisions were required and it appeared that eight iterations were required. The results are shown in Figure 2.5. The correction factor plotted there is the fractional increase due to the edge of the stress intensity factor for an infinite plate with four symmetrically located normal or shear forces.

Figure 2.5

No values of the function $f(b/a)$ were obtained for $b/a < .05$, but the curve plotted in Figure 2.5 seems a reasonable extension of the computed points. The computed points are shown as boxes, and the curve drawn through the points is

$$f(c) = (1-c^2)[0.2945 - 0.3912 c^2 + 0.7685 c^4 - 0.9942 c^6 + 0.5094 c^8] \quad (2.47)$$

This function will be used in a Green's function analysis of the stress intensity factor for an edge crack subjected to some arbitrary distribution of pressure.

One reason for the difficulty in obtaining points on the curve for small values of b/a is the singularity at the point of application of the concentrated load. As long as $b>0$, the stress $\sigma_{xA}^{(0)}(0,y)$ (equation 2.39) has no singularity, and its removal by the half-plane solution of Section 2.2 presents no difficulty. But when $b=0$, the stress on the y -axis has a singularity at the origin which requires special treatment. A straight application of the alternating method to this case would, if the numerical analysis were exactly accurate, give a stress on the crack, $\sigma_{yB}^{(0)}(x,0)$, with a singularity at the origin. Each step of the procedure would leave a stress singularity at the origin. This points up a fundamental difficulty associated with the alternating method in more general cases.

To show the difficulty, recall that equations (2.1) and (2.2) give the solution for the half plane, $y>0$, loaded by normal stresses on the edge, $y=0$. It can be seen from equations (2.2) that

$$\sigma_x(x,0) = \sigma_y(x,0)$$

That is, both normal stresses are the same at each point of the edge. Applying this result to Section 2.3 for arbitrary stress

$$\sigma_{yA}^{(0)}(x,0) = -q^{(0)}(x) = -\sigma(x)$$

on the crack, it is found that the stress, $\sigma_{xA}^{(0)}(0,y)$ satisfies

$$\sigma_{xA}^{(0)}(0,0) = \sigma_{yA}^{(0)}(0,0) \text{ or } p^{(0)}(0) = -q^{(0)}(0).$$

Similarly, in the half plane problem,

$$\sigma_{yB}^{(0)}(0,0) = \sigma_{xB}^{(0)}(0,0) \text{ or } q^{(1)}(0) = -p^{(0)}(0)$$

And so it would continue giving

$$q^{(0)} = -p^{(0)} = q^{(1)} = -p^{(1)} = q^{(2)} = -p^{(3)} = \dots$$

where each function is evaluated at the origin. Therefore,

$$q^{(n)}(0) = q^{(0)}(0) = \sigma(0)$$

After the n^{th} iteration, the superposition of all steps gives the exact solution of the edge crack problem for stress on

the crack given by

$$\sigma_y(x,0) = -\sigma(x) + q^{(n)}(x)$$

And since

$$\sigma_y(0,0) = -\sigma(0) + \sigma(0) = 0$$

the scheme does not converge to the desired solution. That is, $q^{(n)}(x)$ is not negligible compared to $\sigma(x)$ at $x=0$ at least. But no difficulty should be expected if the stress on the edge crack at the edge, $\sigma(0)$, is zero. And in the case of a concentrated force as in equation (2.37) $\sigma(0) = 0$ as long as $b > 0$.

In the case of shear loading, the same difficulty exists. The equality of the normal stresses on the edge and on the plane at right angles to the edge has its counterpart in the obvious statement about the shear stresses on the same planes. The same kind of details could be given for this case, but fundamentally the difficulty is that the shear stress on the crack at the intersection of the crack and edge must be equal to that on the edge unless the stress tensor is allowed to be non-symmetric.

Consider now the case of arbitrary stress on the edge crack,

$$\sigma_y(x,0) = -\sigma(x) , \quad 0 < x < a \quad (2.48)$$

For a concentrated force, $dP = \sigma(x)dx$, located a distance x from the edge, equation (2.45) gives the stress intensity factor

$$dk_1 = \frac{2}{\pi} \sqrt{a} \frac{\sigma(x)dx}{\sqrt{a^2-x^2}} [1+f(x/a)] \quad (2.49)$$

The contribution of each part of the pressure distribution on the crack may be written as in equation (2.49). The total stress intensity factor is obtained by integrating,

$$k_1 = \frac{2}{\pi} \sqrt{a} \left\{ \int_0^a \sigma(x) \frac{dx}{\sqrt{a^2-x^2}} + \int_0^a \sigma(x) \frac{f(x/a)dx}{\sqrt{a^2-x^2}} \right\} \quad (2.50)$$

For shear loading, $\tau_{xy}(x,0) = -\tau(x)$, k_2 is given by the same expression with $\sigma(x)$ replaced by $\tau(x)$. Note that the first term is the stress intensity factor for an infinite plate containing a crack of length $2a$ subjected to the same pressure (even in x). The second term is the correction due to the presence of the free edge. The results of integrating equation (2.50) for a number of pressure variations are contained in the Appendix.

The value of the stress intensity factor listed in Table I was obtained by application of equation (2.50). It may be seen to agree with the value calculated by Koiter [13]. In addition, the other edge crack results in the Appendix agree with those of Lachenbruch [4], though he published only two digit stress intensity factors. The result for linearly varying pressure agrees with that of Stallybrass [18].

3. SURFACE CRACK PROBLEM

One of the crack geometries that has received continual interest in fracture mechanics is that of a semi-elliptical crack whose major axis lies on a stress free surface. This configuration is analogous to the two dimensional version of the edge crack problem discussed earlier except that no reliable method has yet been found to solve the three-dimensional problem. The major cause of difficulty lies in the lack of information at the points where the crack border intersects with the free surface. Sih [22] has discussed this point in detail in connection with the finite thickness crack problem. This difficulty is clearly evidenced by the variation among results [6,9,10] published on the semi-circular and semi-elliptical surface crack problems. In [6,9], the maximum value of the stress-intensity factor was found to be on the free surface, whereas in [10] the maximum occurred at the utmost interior point of the crack front.

In order to demonstrate the sensitivity of the solution to the influence of the free surface the semi-circular crack problem is again treated in this section by the alternating method. With special care given to the stress state around the critical points where the crack border intersects with the free surface, a more accurate numerical solution was achieved. The results are strikingly different from those published in the literature [6,7,8,9,10,23] and are given

for each iteration to illustrate the rate of convergence. The construction of the two sequences used in the alternating method is described in Section 3.3. The general solution used in one sequence is obtained in Section 3.1. The half space solution required by the other sequence is presented in Section 3.2. In Section 3.4, the singularities which affect the numerical solution are discussed, and methods of treating them are given. And, concluding this Section, the numerical results are shown.

3.1 Penny-Shaped Crack in an Infinite Body

The basic solution used for the infinite body containing a penny-shaped crack (Figure 3.1) is obtained from Muki [24]. His solution is valid for completely arbitrary loading of a semi-infinite solid. When the loading is restricted to normal stresses on the surface, his solution may be applied to the case of a penny-shaped crack subjected to arbitrary variation of pressure on its faces. The crack problem may be reduced by symmetry to a half space problem in which known normal stress acts inside a circular region and unknown normal stress (producing known displacement) acts outside this region.

Figure 3.1

A characteristic length is taken to be a , and all length coordinates are expressed as the product of a and a dimensionless coordinate. The cylindrical coordinates (ar , θ , az) shown in Figure 3.1 involve the dimensionless variables r and z . In the following equations, a quantity, p_0 , which has dimensions of stress is shown explicitly so that all quantities appearing after the summation signs are dimensionless. In this Section a will be the radius of the crack and p_0 , the uniform pressure acting on it. In other applications they would designate some other parameters.

If the loading is further restricted to be symmetric about the xz -plane ($\theta=0$), Muki's solution reduces to

$$2\mu u_r = -p_0 a \sum_{m=0}^{\infty} \cos m\theta \int_0^{\infty} [1-2\nu-\xi z] D_m(\xi) e^{-\xi z} [J_{m+1}(\xi r) - \frac{m}{\xi r} J_m(\xi r)] d\xi$$

$$2\mu v_\theta = -p_0 a \sum_{m=0}^{\infty} \sin m\theta \int_0^{\infty} [1-2\nu-\xi z] D_m(\xi) e^{-\xi z} \frac{m}{\xi r} J_m(\xi r) d\xi \quad (3.1)$$

$$2\mu w_z = p_0 a \sum_{m=0}^{\infty} \cos m\theta \int_0^{\infty} [2(1-\nu)+\xi z] D_m(\xi) e^{-\xi z} J_m(\xi r) d\xi$$

for the displacement components, u_r , v_θ , w_z . The shear modulus and Poisson's ratio are denoted by μ and ν , respectively, in equations (3.1). Note that the dimensions of the left hand sides are the same as $p_0 a$. The functions $D_m(\xi)$ remain to be determined by the boundary conditions on $z=0$. The Bessel functions of the first kind, $J_m(\xi r)$, of all integer orders are required in equations (3.1).

The stress components corresponding to the displacement field (3.1) are given by

$$\sigma_r = p_0 \sum_{m=0}^{\infty} \cos m\theta \left\{ - \int_0^{\infty} (1-\xi z) \xi D_m(\xi) e^{-\xi z} J_m(\xi r) d\xi + \frac{1}{r} \int_0^{\infty} (1-2\nu-\xi z) D_m(\xi) e^{-\xi z} \left[\frac{m(m-1)}{\xi r} J_m(\xi r) + J_{m+1}(\xi r) \right] d\xi \right\}$$

$$\sigma_{\theta} = p_0 \sum_{m=0}^{\infty} \cos m\theta \left\{ -2\nu \int_0^{\infty} \xi D_m(\xi) e^{-\xi z} J_m(\xi r) d\xi - \frac{1}{r} \int_0^{\infty} (1-2\nu-\xi z) D_m(\xi) e^{-\xi z} \left[\frac{m(m-1)}{\xi r} J_m(\xi r) + J_{m+1}(\xi r) \right] d\xi \right\}$$

$$\sigma_z = -p_0 \sum_{m=0}^{\infty} \cos m\theta \int_0^{\infty} (1+\xi z) \xi D_m(\xi) e^{-\xi z} J_m(\xi r) d\xi \quad (3.2)$$

$$\tau_{\theta z} = -p_0 \frac{z}{r} \sum_{m=0}^{\infty} m \sin m\theta \int_0^{\infty} \xi D_m(\xi) e^{-\xi z} J_m(\xi r) d\xi$$

$$\tau_{rz} = -p_0 \frac{z}{r} \sum_{m=0}^{\infty} \cos m\theta \int_0^{\infty} \xi D_m(\xi) e^{-\xi z} [\xi r J_{m+1}(\xi r) - m J_m(\xi r)] d\xi$$

$$\begin{aligned} \tau_{r\theta} &= p_0 \frac{1}{r} \sum_{m=0}^{\infty} m \sin m\theta \int_0^{\infty} (1-2\nu-\xi z) D_m(\xi) e^{-\xi z} [J_{m+1}(\xi r) \\ &\quad - \frac{m-1}{\xi r} J_m(\xi r)] d\xi \end{aligned}$$

The shear stresses, $\tau_{\theta z}$ and τ_{rz} , vanish on the plane $z=0$ as required by symmetry about the xy -plane. The boundary conditions of the penny-shaped crack problem which must be satisfied by appropriately choosing $D_m(\xi)$ are

$$\sigma_z = -p_0 p(r, \theta) \text{ on } z=0 \text{ for } r<1 \quad (3.3)$$

$$w_z = 0 \quad \text{on } z=0 \text{ for } r>1$$

where $p(r, \theta)$ is the dimensionless pressure acting on the faces of the crack. Since $p(r, \theta)$ is required to be symmetric about the xz -plane, it may be expanded in a cosine series as

$$p(r, \theta) = \sum_{m=0}^{\infty} K_m(r) \cos m\theta \quad (3.4)$$

where $K_0(r) = \frac{1}{\pi} \int_0^{\pi} p(r, \theta) d\theta$

$$K_m(r) = \frac{2}{\pi} \int_0^{\pi} p(r, \theta) \cos m\theta d\theta , \quad m \geq 1 \quad (3.5)$$

The equations for $D_m(\xi)$ are obtained by using equations (3.3) in conjunction with (3.1), (3.2), (3.4).

They are

$$\begin{aligned} \int_0^{\infty} \xi D_m(\xi) J_m(\xi r) d\xi &= K_m(r) , \quad r < 1 \\ \int_0^{\infty} D_m(\xi) J_m(\xi r) d\xi &= 0 , \quad r > 1 \end{aligned} \quad (3.6)$$

for each $m = 0, 1, 2, \dots$. The procedure for solving these

equations is analogous to that in Section 2.1. The displacement-like function,

$$w_m(r) = \int_0^\infty D_m(\xi) J_m(\xi r) d\xi \quad (3.7)$$

is introduced. Since by the second of equations (3.6), $w_m(r) = 0$ for $r > 1$, the Hankel inverse transform [15] of equation (3.7) is

$$D_m(\xi) = \xi \int_0^1 w_m(r) J_m(\xi r) dr \quad (3.8)$$

The displacement-like behavior of $w_m(\xi)$ is assured if it is represented in the form

$$w_m(r) = \frac{2}{\pi} r^m \int_r^1 g_m(t) \frac{t^{-m+1} dt}{\sqrt{t^2 - r^2}} \quad (3.9)$$

Use of equation (3.9) in equation (3.8) gives another representation of $D_m(\xi)$,

$$\begin{aligned} D_m(\xi) &= \frac{2}{\pi} \xi \int_0^1 J_m(\xi r) r^m dr \int_r^1 g_m(t) \frac{t^{-m+1} dt}{\sqrt{t^2 - r^2}} \\ &= \frac{2}{\pi} \xi \int_0^1 t^{-m+1} g_m(t) dt \int_0^t r^{m+1} \frac{J_m(\xi r) dr}{\sqrt{t^2 - r^2}} \\ &= \frac{2}{\pi} \xi \int_0^1 t^2 g_m(t) j_m(\xi t) dt \end{aligned} \quad (3.10)^*$$

* The formula at the top of page 32 of [20] may be used in the last step if the substitution, $r = ts \sin \theta$ is made.

$$\text{where } j_m(\xi t) = \sqrt{\frac{\pi}{2\xi t}} J_{m+\frac{1}{2}}(\xi t)$$

is the spherical Bessel function of the first kind of order m .

If the first of equations (3.6) is multiplied on both sides by r^{m+1} , it can be integrated with respect to r to become

$$\int_0^\infty D_m(\xi) r^{m+1} J_{m+1}(\xi r) d\xi = L_m(r), \quad r < 1 \quad (3.11)$$

$$\text{where } L_m(r) = \int_0^r n^{m+1} K_m(n) dn \quad (3.12)$$

The equation which determines $g_m(t)$ is obtained by substituting equation (3.10) into (3.11):

$$\begin{aligned} \frac{2}{\pi} \int_0^\infty \xi J_{m+1}(\xi r) d\xi \int_0^1 t^2 g_m(t) j_m(\xi t) dt &= r^{-m-1} L_m(r), \quad r < 1 \\ \text{or } \int_0^1 t^2 g_m(t) dt \int_0^\infty \xi J_{m+1}(\xi r) j_m(\xi t) d\xi &= \frac{\pi}{2} r^{-m-1} L_m(r), \quad r < 1 \end{aligned} \quad (3.13)$$

Knowing that*

$$\int_0^\infty \xi J_{m+1}(\xi r) j_m(\xi t) d\xi = \begin{cases} 0 & , \quad t > r \\ \frac{t^m r^{-m-1}}{\sqrt{r^2 - t^2}} & , \quad t < r \end{cases}$$

equation (3.13) may be written as

$$\int_0^r g_m(t) \frac{t^{m+2} dt}{\sqrt{r^2 - t^2}} = \frac{\pi}{2} L_m(r), \quad r < 1 \quad (3.14)$$

*Third formula on page 37 of [20] with $\mu=m$, $v=m+\frac{1}{2}$

By application of the solution, equation (2.14), of equation (2.13) to equation (3.14),

$$t^{m+2}g_m(t) = t \int_0^t \frac{L'_m(r)dr}{\sqrt{t^2-r^2}}$$

or, since equation (3.12) gives

$$L'_m(r) = r^{m+1}K_m(r)$$

$$g_m(t) = t^{-m-1} \int_0^t K_m(r) \frac{r^{m+1}dr}{\sqrt{t^2-r^2}} \quad (3.15)$$

Changing the variable of integration in equation (3.15) from r to $\zeta = r/t$ gives the form,

$$g_m(t) = \int_0^1 K_m(t\zeta) \frac{\zeta^{m+1}d\zeta}{\sqrt{1-\zeta^2}}$$

The stress intensity factor is most conveniently determined by examining the crack opening shape near $r=1$. From equations (3.1), (3.7) the displacement for $z=0$ is

$$w_z = \frac{1-\nu}{\mu} p_0 a \sum_{m=0}^{\infty} w_m(r) \cos m\theta \quad (3.16)$$

For $r=1-\rho$, equation (3.9) becomes

$$\begin{aligned} w_m(1-\rho) &= \frac{2}{\pi} (1-\rho)^m \int_{1-\rho}^1 g_m(t) \frac{t^{-m+1}dt}{\sqrt{t^2-(1-\rho)^2}} \\ &= \frac{2}{\pi} (1-\rho)^m \int_0^\rho g_m(1-\eta) \frac{(1-\eta)^{-m+1}d\eta}{\sqrt{\rho-\eta} \sqrt{2-\rho-\eta}} \end{aligned}$$

As $\rho \rightarrow 0$, ρ and η may be neglected in comparison with 1, and this leads to

$$\begin{aligned} w_m(1-\rho) &= \frac{2}{\pi} g_m(1) \frac{1}{\sqrt{2}} \int_0^\rho \frac{d\eta}{\sqrt{\rho-\eta}} + O(\rho) \\ &= \frac{2}{\pi} g_m(1) \sqrt{2\rho} + O(\rho) \end{aligned}$$

Therefore, the equation (3.16) for the crack opening near the crack front becomes

$$w_z = \frac{2(1-v^2)}{\pi E} p_0 \sqrt{a} \sqrt{2ap} \sum_{m=0}^{\infty} g_m(1) \cos m\theta + O(\rho) \quad (3.17)$$

The relationship between displacement and stress intensity factor (See equation (5.37) of [21]) is the same as in equation (2.16) for plane strain. In equation (2.16), note that r is not dimensionless. Hence it is identified with ap in equation (3.17). Thus, comparing equations (3.17) and (2.16),

$$k_p = \frac{2}{\pi} p_0 \sqrt{a} \sum_{m=0}^{\infty} g_m(1) \cos m\theta \quad (3.18)$$

In equation (3.18), k_p is the physically dimensioned stress intensity factor. The subscript p is used to distinguish it from the dimensionless stress intensity factor

$$k(\theta) = \sum_{m=0}^{\infty} g_m(1) \cos m\theta = k_p / \left(\frac{2}{\pi} p_0 \sqrt{a} \right) \quad (3.19)$$

which will be used in the numerical calculations.

The stress intensity factor may also be determined by calculating the singular part of the stress distribution. If equation (3.10) is integrated by parts,

$$D_m(\xi) = \frac{2}{\pi} g_m(1) j_{m+1}(\xi) - \frac{2}{\pi} \int_0^1 t^{m+2} j_{m+1}(\xi t) \frac{d}{dt} [t^{-m} g_m(t)] dt$$

only the first term contributes to the stress singularities.

The spherical Bessel functions may be written as the product of polynomials in $\frac{1}{\xi}$ and trigonometric functions as e.g.

$$j_0(\xi) = \frac{\sin \xi}{\xi}, \quad j_1(\xi) = \frac{\sin \xi}{\xi^2} - \frac{\cos \xi}{\xi}$$

The resulting integrals of the type

$$\int_0^\infty \xi^n e^{-\xi z} J_m(\xi r) \sin \xi d\xi$$

obtained from equations (3.2) may be evaluated from formulas based on the third one on page 33 of [20]. By differentiating and separating the real and imaginary parts of the formula referred to, results of the type

$$\int_0^\infty e^{-\xi z} J_m(\xi r) \sin \xi d\xi = \frac{r^{-m}}{\sqrt{2\rho}} \sin\left(\frac{\phi}{2} + \frac{m\pi}{2}\right) + O(1)$$

are found. After these results are used, and the nonsingular terms discarded, the stress state may be written in the form,

$$\sigma_r = \frac{2}{\pi} p_0 \frac{k(\theta)}{\sqrt{2\rho}} \left[\cos\frac{\phi}{2} - \frac{1}{2} \sin\phi \sin\frac{3\phi}{2} \right] + O(1)$$

$$\begin{aligned}\sigma_{\theta} &= 2\nu \frac{2}{\pi} p_0 \frac{k(\theta)}{\sqrt{2\rho}} [\cos \frac{\phi}{2}] + o(1) \\ \sigma_z &= \frac{2}{\pi} p_0 \frac{k(\theta)}{\sqrt{2\rho}} [\cos \frac{\phi}{2} + \frac{1}{2} \sin \phi \sin \frac{3\phi}{2}] + o(1) \\ \tau_{rz} &= -\frac{2}{\pi} p_0 \frac{k(\theta)}{\sqrt{2\rho}} [\frac{1}{2} \sin \phi \cos \frac{3\phi}{2}] + o(1)\end{aligned}\quad (3.20)$$

In equations (3.20), ρ and ϕ are the dimensionless polar coordinates shown in Figure 3.2. The stresses $\tau_{\theta z}$ and $\tau_{r\theta}$, are nonsingular. It may be verified that the singular terms satisfy the condition of plane strain,

$$\sigma_{\theta} = \nu(\sigma_r + \sigma_z)$$

locally.

Figure 3.2

The present iterative approach requires the calculation of the stresses on the yz -plane. In general each of the stresses, σ_x , τ_{xy} , τ_{xz} , is not zero, but for the case in which the pressure on the crack is symmetric about the yz -plane, only the normal stress is not zero. It may be evaluated from equations (3.2) by

$$\sigma_x(0, y, z) = \sigma_{\theta}(y, \pi/2, z)$$

It is helpful in the numerical analysis to separate the singular and nonsingular parts of this stress as

$$\sigma_x = 2\nu \frac{2}{\pi} p_0 k\left(\frac{\pi}{2}\right) \left[\frac{1}{\sqrt{2\rho_1}} \cos \frac{\phi_1}{2} + \frac{1}{\sqrt{2\rho_2}} \cos \frac{\phi_2}{2} \right] + p_0 q(y, z) \quad (3.21)$$

where (ρ_1, ϕ_1) and (ρ_2, ϕ_2) are coordinates in the yz -plane as shown in Figure 3.4. The nonsingular function $q(y, z)$ is computed from the preceding two equations as long as the point $(0, y, z)$ is not close to the crack front. When $(0, y, z)$ nears one of the points $(0, \pm a, 0)$, the singular parts of equations (3.21) and (3.22) are equal, and $q(y, z)$ may be written in a form in which the singularities are analytically cancelled. From equations (3.2) and (3.21),

$$\begin{aligned} q(y, z) = & - \frac{4\nu}{\pi} k\left(\frac{\pi}{2}\right) \left[\frac{1}{\sqrt{2\rho_1}} \cos \frac{\phi_1}{2} + \frac{1}{\sqrt{2\rho_2}} \cos \frac{\phi_2}{2} \right] \\ & + \sum_{m=0}^{\infty} (-1)^m \left\{ -2\nu \int_0^{\infty} \xi D_{2m}(\xi) e^{-\xi z} J_{2m}(\xi y) d\xi \right. \\ & - \frac{1}{y} \int_0^{\infty} (1-2\nu-\xi z) D_{2m}(\xi) e^{-\xi z} \left[\frac{2m(2m-1)}{\xi y} \right] J_{2m}(\xi y) \right. \\ & \left. \left. + J_{2m+1}(\xi y) \right] d\xi \right\} \end{aligned} \quad (3.22)$$

Use has been made of the fact that for symmetry of loading about the yz -plane, all K , g , D with odd subscripts vanish.

To illustrate the lack of singularity in $q(y, z)$, the form valid for $z=0$ and $y \leq 1$ will be given. A similar expression can be written for $y \geq 1$, and at $y=1$, both give the same value of $q(y, z)$. The Fourier coefficients of $p(r, \theta)$ can be written as polynomials,

$$K_0(r) = p_c + \sum_{n=1}^N A_{1n} r^n$$

$$K_{2m}(r) = \sum_{n=1}^N A_{m+1,n} r^n , \quad m \geq 1 \quad (3.23)$$

where $p_c = K_0(0) = p(0, \theta)$ is the dimensionless pressure at the center of the crack. For $K_{2m}(r)$ in this form, equation (3.15) gives

$$g_0(t) = p_c + \sum_{n=1}^N c_{1n} t^n$$

$$g_{2m}(t) = \sum_{n=1}^N c_{m+1,n} t^n , \quad m \geq 1 \quad (3.24)$$

$$\text{where } c_{mn} = I_{2m+n-1} A_{mn} \quad (3.25)$$

$$\text{and } I_0 = \frac{\pi}{2} , \quad I_1 = 1 , \quad I_k = \frac{k-1}{k} I_{k-2} \quad (3.26)$$

The part of $D_0(\xi)$ resulting from the constant part of $g_0(t)$ may be evaluated as

$$\frac{2}{\pi} \xi \int_0^1 t^2 p_c j_0(\xi t) dt = p_c j_1(\xi)$$

and the integrals of this part of $D_0(\xi)$ in equation (3.22) can be determined in closed form. The remaining part of $D_0(\xi)$ and the other $D_{2m}(\xi)$ can be found in terms of spherical Bessel functions and the sine integral function. In general, the remaining integrals in equation (3.22) are evaluated numerically, but when $z=0$ they can be explicitly obtained.

For $z=0$ and $y \leq 1$, the integrations in equation (3.22) result in

$$q(y, 0) = \frac{2}{\pi} p_c F_0(y, 0) + \frac{2}{\pi} \sum_{m=1}^{\infty} (-1)^m \sum_{n=1}^N I_{2m+n} C_{mn} y^n [1 - 2v + 2v(2m+n) + (1-2v)(2m-2)(2m-3) F_{mn}(y)] \quad (3.27)$$

where

$$F_{mn}(y) = \begin{cases} \frac{1 - \frac{I_{4m-4}}{I_{2m+n}} y^{2m-4+n}}{2m-4-n}, & n \neq 2m-4 \\ \ln \frac{y}{2} + \frac{1}{1 \cdot 2} + \frac{1}{3 \cdot 4} + \dots + \frac{1}{(4m-5)(4m-4)}, & n = 2m-4 \end{cases}$$

A similar but more complicated result can be found for $y \geq 1$. Using the polar coordinates shown in Figure 3.4, the other function in equation (3.27) may be written

$$\begin{aligned} F_0(y, z) = & 2v \left[\frac{1}{\sqrt{\rho_1 \rho_2}} \sin \frac{\phi_1 + \phi_2}{2} - \frac{1}{\sqrt{2\rho_1}} \cos \frac{\phi_1}{2} - \frac{1}{\sqrt{2\rho_2}} \cos \frac{\phi_2}{2} \right] \\ & - \frac{1+2v}{2} \arcsin \left(\frac{2}{\rho_1 + \rho_2} \right) + \frac{1-2v}{2y^2} \sqrt{\rho_1 \rho_2} \left[\sin \frac{\phi_1 + \phi_2}{2} \right. \\ & \left. + z \cos \frac{\phi_1 + \phi_2}{2} \right] + \frac{z}{y^2 \sqrt{\rho_1 \rho_2}} \left[z \sin \frac{\phi_1 + \phi_2}{2} \right. \\ & \left. + (\rho_1 \rho_2 - 1) \cos \frac{\phi_1 + \phi_2}{2} \right] \end{aligned} \quad (3.28)$$

For $z=0$, equation (3.28) reduces to

$$F_0(y, 0) = - \frac{v\sqrt{2(y-1)}}{\sqrt{2(y+1)+y+1}} - \frac{1+2v}{2} \arcsin \frac{1}{y} + \frac{1-2v}{2y} \sqrt{y^2 - 1} \quad (3.29)$$

for $y \geq 1$. For $y < 1$, $F_0(y, 0)$ is equal to the constant obtained from equation (3.29) by putting $y=1$.

Reiterating the important results, if $p(r, \theta)$ is symmetric about both the xz - and the yz -planes, then it can be written

$$p(r, \theta) = -\frac{1}{p_0} \sigma_z(x, y, 0) = \sum_{m=0}^{\infty} K_{2m}(r) \cos 2m\theta \quad (3.30)$$

It follows that

$$g_{2m}(t) = \int_0^1 \zeta^{2m+1} \frac{K_{2m}(\zeta t) dt}{\sqrt{1-\zeta^2}} \quad (3.31)$$

can be computed to yield the stress intensity factor

$$k_p(\theta) = \frac{2}{\pi} p_0 \sqrt{a} \sum_{m=0}^{\infty} g_{2m}(1) \cos 2m\theta \quad (3.32)$$

and

$$D_{2m}(\xi) = \frac{2}{\pi} \xi \int_0^1 t^2 g_{2m}(t) j_{2m}(\xi t) dt. \quad (3.33)$$

Once $D_{2m}(\xi)$ is computed, any of the stresses and displacements may be determined. In particular $\sigma_x(0, y, z)$ of equation (3.21) is obtained by calculating the function $q(y, z)$ from eq.(3.22).

3.2 Surface Loads on Half Space

(1) Nonsingular stress

Consider the case of normal stresses σ_x acting on the surface occupying the yz -plane as shown in Figure 3.3.

For the case

$$\sigma_x(0,y,z) = p_0 q(y,z) \quad (3.34)$$

in which there is no stress singularity, there are a number of possible methods of solution. For example, the solution at the beginning of Section 3.1 could be applied or the solution for a concentrated force on a half space could be used as a Green's function. For the convenience of numerical calculation as in [6], the surface will be divided into squares sufficiently small in size so that the stress is nearly uniform on each. Next a solution provided by Love [25] is used to obtain the contribution of the stress σ_x on each square to the stress σ_z on the xy plane.

Figure 3.3

Love's solution gives the normal stress σ_z on the xy-plane due to a unit tensile stress on a square of side b centered at $(0, \bar{y}, \bar{z})$ as

$$\sigma_z(x, y, 0) = F(|\bar{y} - y|, |\bar{z}|, |x|)$$

where $2\pi F(\xi, \eta, \zeta) = (1-2\nu)F_1(\xi, \eta, \zeta) - \zeta F_2(\xi, \eta, \zeta) - 2\nu F_3(\xi, \eta, \zeta)$ (3.35)

and the functions F_j ($j=1, 2, 3$) stand for

$$F_1 = \tan^{-1} \frac{b-\xi}{b-\eta} + \tan^{-1} \frac{b+\xi}{b-\eta} - \tan^{-1} \frac{\zeta(b-\xi)}{a_1(b-\eta)} - \tan^{-1} \frac{\zeta(b+\xi)}{b_2(b-\eta)} \\ + \tan^{-1} \frac{b-\xi}{b+\eta} + \tan^{-1} \frac{b+\xi}{b+\eta} - \tan^{-1} \frac{\zeta(b-\xi)}{d_4(b+\eta)} - \tan^{-1} \frac{\zeta(b+\xi)}{c_3(b+\eta)}$$

$$F_2 = \frac{b-\eta}{(b-\eta)^2 + \zeta^2} \left[\frac{b-\xi}{a_1} + \frac{b+\xi}{b_2} \right] + \frac{b+\eta}{(b+\eta)^2 + \zeta^2} \left[\frac{b-\xi}{d_4} + \frac{b+\xi}{c_3} \right] \quad (3.36)$$

$$F_3 = \tan^{-1} \frac{\zeta a_1}{(b-\xi)(b-\eta)} + \tan^{-1} \frac{\zeta b_2}{(b+\xi)(b-\eta)} \\ + \tan^{-1} \frac{\zeta c_3}{(b+\xi)(b+\eta)} + \tan^{-1} \frac{\zeta d_4}{(b-\xi)(b+\eta)} - \begin{cases} 2\pi, & |\xi| < b, |\eta| < b \\ 0, & \text{otherwise} \end{cases}$$

with the following contractions

$$a_1^2 = (b-\xi)^2 + (b-\eta)^2 + \zeta^2$$

$$b_2^2 = (b+\xi)^2 + (b-\eta)^2 + \zeta^2$$

$$c_3^2 = (b+\xi)^2 + (b+\eta)^2 + \zeta^2$$

$$d_4^2 = (b-\xi)^2 + (b+\eta)^2 + \zeta^2$$

By taking advantage of symmetry, attention may be confined to the centers $(0, \bar{y}_i, \bar{z}_j)$ of the squares which lie in the first quadrant of the yz -plane. The effect of the other three symmetrically located quadrants is included in the result

$$\sigma_z(x, y, 0) = p_0 t(x, y)$$

where

$$t(x, y) = 2 \sum_{i=1}^N \sum_{j=1}^N q(\bar{y}_i, \bar{z}_j) [F(|\bar{y}_i - y|, |\bar{z}_j|, |x|) \\ + F(|\bar{y}_i + y|, |\bar{z}_j|, |x|)] \quad (3.37)$$

The symmetry of the stress on the yz -plane insures that there will be no shear stresses on the xy -plane.

Figure 3.4

(2) Singular stress

When the stress on the yz -plane is singular, it is desirable to seek a closed form solution. For the case of interest, from equation (3.21),

$$\sigma_x(0, y, z) = \frac{4\nu}{\pi} p_0 k\left(\frac{\pi}{2}\right) \left[\frac{1}{\sqrt{2\rho_1}} \cos \frac{\phi_1}{2} + \frac{1}{\sqrt{2\rho_2}} \cos \frac{\phi_2}{2} \right] \quad (3.38)$$

such a solution can be found by applying Muki's half-space solution, equations (3.1) and (3.2), to each term. The result is

$$\sigma_z(x, y, 0) = \frac{4\nu}{\pi} p_0 k\left(\frac{\pi}{2}\right) \left[\frac{1}{\sqrt{2R_1}} S(\psi_1) + \frac{1}{\sqrt{2R_2}} S(\psi_2) \right] \quad (3.39)$$

where the dimensionless coordinates, ρ , ϕ , R , ψ are shown in Figure 3.4. The function $S(\psi)$ is in the form of an infinite series involving hypergeometric functions. Rather than give the formulas, the results are shown graphically in Figure 3.5. An excellent fit of the exactly computed points of the curve is obtained by the approximation,

$$\begin{aligned} S(\psi) = & \sqrt{\psi} [0.344 + 1.851\psi - 11.637\psi^2 + 34.545\psi^3 \\ & - 61.286\psi^4 + 68.124\psi^5 - 47.644\psi^6 + 20.321\psi^7 \\ & - 4.823\psi^8 + 0.488\psi^9] \end{aligned} \quad (3.40)$$

This expression is valid only for $0 \leq \psi \leq \pi/2$ and for Poisson's ratio, $\nu = 0.30$.

Figure 3.5

It should be noted that there are singularities in $\sigma_z(x, y, 0)$ at the points where the crack front intersects the free surface. The numerical difficulties due to the singularity will be discussed in more detail in Section 3.4.

3.3 Iterative Formulation

The solutions of the two preceding problems will be superposed alternately to solve the case of a uniformly pressurized half penny-shaped crack perpendicular to a free surface (Figure 3.6). The procedure begins with the well known solution [26] for uniform pressure of a penny-shaped crack in an infinite medium. This solution gives stresses on the yz -plane which are removed by superposing the half space solution for equal and opposite stresses on the yz -plane. As a result of the half space solution, there is a residual normal stress on the crack in addition to the uniform pressure. This is eliminated by superposing the solution of Section 3.1 for pressure on the crack equal to the residual stress. Again, stresses on the yz -plane are produced which are removed by application of the half space solution. The cycle of superpositions is continued until the residual stress on the crack is negligible compared to the uniform pressure.

Figure 3.6

As outlined, the first step in the procedure requires the solution of the penny-shaped crack problem for the case

$$\sigma_{zA}^{(0)}(x, y, 0) = -p_0 \quad (3.41)$$

Either [26] or Section 3.1 may be used to find the stress intensity factor,

$$k_p^{(0)} = \frac{2}{\pi} p_0 \sqrt{a} \quad \text{or} \quad k^{(0)}(\theta) = 1 \quad (3.42)$$

and the stress on the yz -plane,

$$\begin{aligned} \sigma_{xA}^{(0)}(0, y, z) &= \frac{4\nu}{\pi} p_0 k^{(0)}\left(\frac{\pi}{2}\right) \left[\frac{1}{\sqrt{2\rho_1}} \cos \frac{\phi_1}{2} + \frac{1}{\sqrt{2\rho_2}} \cos \frac{\phi_2}{2} \right] \\ &+ p_0 q^{(0)}(y, z) \end{aligned} \quad (3.43)$$

See Figure 3.4 for the coordinates, ρ, ϕ . For the case of uniform pressure, $q^{(0)}(y, z)$ is equal to $\frac{2}{\pi} F_0(y, z)$ which is given in equation (3.28).

The second half of the zeroth iteration is used to eliminate the stress on the free surface. The stress applied to the surface is

$$\sigma_{xB}^{(0)}(0, y, z) = \sigma_{xA}^{(0)}(0, y, z) \quad (3.44)$$

which gives the result (See Figure 3.4 for R, ψ .)

$$\sigma_{zB}^{(0)}(x, y, 0) = \frac{4\nu}{\pi} p_0 k^{(0)}\left(\frac{\pi}{2}\right) \left[\frac{S(\psi_1)}{\sqrt{2R_1}} + \frac{S(\psi_2)}{\sqrt{2R_2}} \right] + p_0 t^{(1)}(x, y) \quad (3.45)$$

where $t^{(1)}(x,y)$ is determined by applying the method of Section 3.2(1). It depends only on $q^{(0)}$, and not on the singular part of $\sigma_{xA}^{(0)}$.

After the second half of this iteration is subtracted from the first half, the surface will be free of stress, but the stress on the crack will be

$$\sigma_z(x,y,0) = -p_0 - \sigma_{zB}^{(1)}(x,y,0) \quad (3.46)$$

rather than constant. An additional iteration is used to eliminate the stress $\sigma_{zB}^{(0)}$.

For the first iteration, the stress on the penny-shaped crack is taken to be

$$\begin{aligned} \sigma_{zA}^{(1)}(x,y,0) &= \sigma_{zB}^{(0)}(x,y,0) = \frac{4\nu}{\pi} p_0 k^{(0)}\left(\frac{\pi}{2}\right) \left[\frac{s(\psi_1)}{\sqrt{2R_1}} + \frac{s(\psi_2)}{\sqrt{2R_2}} \right] \\ &\quad + p_0 t^{(1)}(x,y) \end{aligned} \quad (3.47)$$

Because of the singularity in the first term of equation (3.47), care must be taken in the numerical procedure. The description of the numerical method will be given in the following section. The contribution of the two parts of $\sigma_{zA}^{(1)}$ are computed separately and the desired quantities expressed as

$$k^{(1)}(\theta) = \frac{4\nu}{\pi} k^{(0)}\left(\frac{\pi}{2}\right) k_S(\theta) + k_N^{(1)}(\theta) \quad (3.48)$$

$$q^{(1)}(y,z) = \frac{4\nu}{\pi} k^{(0)}\left(\frac{\pi}{2}\right) q_S(y,z) + q_N^{(1)}(y,z) \quad (3.49)$$

$$\begin{aligned}\sigma_{xA}^{(1)}(0,y,z) &= \frac{4v}{\pi} p_0 k^{(1)}\left(\frac{\pi}{2}\right) \left[\frac{1}{\sqrt{2\rho_1}} \cos \frac{\phi_1}{2} + \frac{1}{\sqrt{2\rho_2}} \cos \frac{\phi_2}{2} \right] \\ &+ p_0 q^{(1)}(y,z)\end{aligned}\quad (3.50)$$

where $k_S(\theta)$ and $p_0 q_S(y,z)$ are the dimensionless stress intensity factor and nonsingular part of $\sigma_x(0,y,z)$, respectively, due to stress on the crack of

$$\sigma_z(x,y,0) = p_0 \left[\frac{s(\psi_1)}{\sqrt{2R_1}} + \frac{s(\psi_2)}{\sqrt{2R_2}} \right] \quad (3.51)$$

Similarly, $k_N^{(1)}(\theta)$ and $p_0 q_N^{(1)}(y,z)$ stem from the stress $p_0 t^{(1)}(x,y)$ on the crack.

The effects of these two terms are kept separate into the second half of the iteration. The stress on the half space is taken to be

$$\sigma_{xB}^{(1)}(0,y,z) = \sigma_{xA}^{(1)}(0,y,z)$$

This results in the residual stress on the crack,

$$\sigma_{zB}^{(1)}(x,y,0) = \frac{4v}{\pi} p_0 k^{(1)}\left(\frac{\pi}{2}\right) \left[\frac{s(\psi_1)}{\sqrt{2R_1}} + \frac{s(\psi_2)}{\sqrt{2R_2}} \right] + p_0 t^{(2)}(x,y) \quad (3.52)$$

where

$$t^{(2)}(x,y) = \frac{4v}{\pi} k^{(0)}\left(\frac{\pi}{2}\right) t_S(x,y) + t_N^{(2)}(x,y) \quad (3.53)$$

In a way similar to the definitions of q_S and $q_N^{(1)}$, t_S and $t_N^{(2)}$ are defined to be the stress $\sigma_z(x,y,0)$ due to the stress

$\sigma_x(0,y,z)$ equal to q_S and $q_N^{(1)}$, respectively, and are found by the method of Section 3.2(1).

Again, the second half of the iteration when subtracted from the first half frees the surface of stresses. Adding the first iteration to the zeroth cancels the residual stress $\sigma_{zB}^{(0)}$ and gives

$$\sigma_z(x,y,0) = -p_0 - \sigma_{zB}^{(1)}(x,y,0)$$

Further iterations are added until the stress on the crack is reduced to the applied stress $-p_0$ to within some arbitrary tolerance. The additional computations which must be made for each iteration are straightforward. For the second iteration, the dimensionless intensity factor, $k_N^{(2)}(\theta)$, and stress $\sigma_x(0,y,z) = p_0 q_N^{(2)}(y,z)$ due to stress on the crack of $\sigma_z(x,y,0) = p_0 t^{(2)}(x,y)$ are obtained. Then the half space solution gives $\sigma_z(x,y,0) = p_0 t_N^{(3)}(x,y)$ due to $\sigma_x(0,y,z) = p_0 q_N^{(2)}(y,z)$. The contribution of this iteration to the dimensionless stress intensity factor is

$$k^{(2)}(\theta) = \frac{4v}{\pi} k^{(1)}\left(\frac{\pi}{2}\right) k_S(\theta) + k_N^{(2)}(\theta)$$

and the stress on the crack is

$$\sigma_z(x,y,0) = -p_0 - \sigma_{zB}^{(2)}(x,y,0)$$

where

$$\sigma_{zB}^{(2)} = \frac{4v}{\pi} p_0 k^{(2)}\left(\frac{\pi}{2}\right) \left[\frac{S(\psi_1)}{\sqrt{2R_1}} + \frac{S(\psi_2)}{\sqrt{2R_2}} \right] + p_0 t^{(3)}(x,y)$$

$$t^{(3)}(x,y) = \frac{4v}{\pi} k^{(1)}\left(\frac{\pi}{2}\right) t_S(x,y) + t_N^{(3)}(x,y)$$

For the n^{th} iteration, the functions, $k_S(\theta)$, $q_S(y,z)$, and $t_S(x,y)$, are used again in conjunction with the results of the previous iteration, $k^{(n-1)}(\theta)$ and $t^{(n)}(x,y)$. The method of Section 3.1 gives the new functions, $k_N^{(n)}(\theta)$ and $q_N^{(n)}(y,z)$, which are, respectively, the dimensionless stress intensity factor and the nonsingular part of $\sigma_x(0,y,z)$ produced by application of the stress $\sigma_z(x,y,0) = t^{(n)}(x,y)$ to the crack. The half space solution of Section 3.2(1) gives $t_N^{(n+1)}(x,y)$, the stress $\sigma_z(x,y,0)$ produced by $\sigma_x(0,y,z) = q_N^{(n)}(y,z)$ acting on the surface. The new addition to the dimensionless stress intensity factor is

$$k^{(n)}(\theta) = \frac{4v}{\pi} k^{(n-1)}\left(\frac{\pi}{2}\right) k_S(\theta) + k_N^{(n)}(\theta)$$

and the residual stress on the crack is

$$\sigma_{zB}^{(n)}(x,y,0) = \frac{4v}{\pi} p_0 k^{(n)}\left(\frac{\pi}{2}\right) \left[\frac{S(\psi_1)}{\sqrt{2R_1}} + \frac{S(\psi_2)}{\sqrt{2R_2}} \right] + p_0 t^{(n+1)}(x,y)$$

where the term carried into the next iteration, if necessary, is

$$t^{(n+1)}(x,y) = \frac{4v}{\pi} k^{(n-1)}\left(\frac{\pi}{2}\right) t_S(x,y) + t_N^{(n+1)}(x,y)$$

The alternating method applied in this Section is modified by the separate treatment of the singular part of the stress (equation (3.43)) applied to the half space. The solution for the half space subjected to the singular stress

is given by the first part of equation (3.45). The resulting stress which must be removed from the crack, eq. (3.47), has two parts which are kept separate. The singular part is the same in each iteration except for the coefficient involved. Therefore, the numerical solution for a penny-shaped crack subjected to the singular stress (tensile) of equation (3.51) is determined to as high a degree of accuracy as possible. The contribution of this solution to each iteration is contained in the functions with a subscript, S. The remaining contribution, from the rest of equation (3.47) gives the terms denoted by the subscript, N. The parts are combined as in equations (3.48) to (3.50) to give the total solution of the penny-shaped crack problem for this iteration. The solution is treated by the same method in each successive iteration.

The next section contains a description of the numerical details and the difficulties associated with the stress singularity of equation (3.47).

3.4 Numerical Treatment of Singularities

(1) Half space

For the case of uniform pressure on the crack, the first step requiring numerical analysis is the clearing of the stress, eq.(3.43) from the surface in the second half of the zeroth iteration. For convenience the problem is a half space with tensile stresses,

$$\sigma_x(0,y,z) = p_0 q(y,z)$$

on the surface. The function $q(y,z)$ can be any of the non-singular functions of the first line of Table II. The solution for the singular part of the stress $\sigma_x(0,y,z)$ is given analytically by equations (3.38) to (3.40).

The surface of the half space is divided into a number of regions as shown in Figure 3.7. Each region is then subdivided into a number of squares, larger squares being used where the stress becomes small and less rapidly varying. The values of $q^{(0)}(y,z)$ at the centers of each of the squares are computed from the closed form expression, equation (3.28). Because of the lengthy calculations needed to obtain the values of the other q 's, they were computed at fewer points and the six point bivariate interpolation formula was used to get the values at the remaining points. The numbers in parentheses in Figure 3.7 give the number of values of y and the number of values of z , respectively, used to obtain the grid points at which q was calculated exactly. After the values of $q(y,z)$ have been computed at the center of each square, the solution in Section 3.2(1) is used directly to obtain the values of the stress on the xy -plane denoted by

$$\sigma_z(x,y,0) = p_0 t(x,y) \quad (3.54)$$

where the t 's corresponding to the various q 's are shown in Table II.

Table II: Results of Half Space Solution
of Section 3.2(1).

			$n \geq 1$
surface stress $\sigma_x(0,y,z)/p_0 =$	$q^{(0)}(y,z)$	$q_S(y,z)$	$q_N^{(n)}(y,z)$
results in $\sigma_z(x,y,0)/p_0 =$	$t^{(1)}(x,y)$	$t_S(x,y)$	$t_N^{(n+1)}(x,y)$

The values of $t(x,y)$ are computed at the 36 points $(.2m, .2n)$, $m,n=0,1,\dots,5$. The six point bivariate interpolation formula is used to obtain intermediate values of $t(x,y)$. This completes the description of the half space problem's numerical solution.

(2) Penny-shaped crack--nonsingular load

The solution of the penny-shaped crack problem is needed for stresses on the crack which contain no singularities.

$$\sigma_z(x,y,0) = p_0 t(x,y)$$

The function $t(x,y)$ may represent any of the t 's in Table III. In a case of non-uniform pressure on the crack, it could also represent the initial stress on the crack, $t^{(0)}(x,y)$. (In this example, $t^{(0)}(x,y) = -1$). As indicated above, $t(x,y)$ is known at 36 points and interpolation gives its value at any other point on the crack.

The solution of Section 3.1 requires first the computation of the Fourier coefficients of

$$p(r, \theta) = -t(x, y)$$

which are

$$\begin{aligned} K_0(r) &= \frac{2}{\pi} \int_0^{\pi/2} p(r, \theta) d\theta \\ K_{2m}(r) &= \frac{4}{\pi} \int_0^{\pi/2} p(r, \theta) \cos 2m\theta d\theta, \quad m \geq 1 \end{aligned} \quad (3.55)$$

$$K_{2m+1}(r) = 0, \quad m \geq 0$$

The first 40 K's are each computed for 30 values of r using a technique given by Filon [27]. His technique gives as good accuracy with 100 divisions of the range of integration as the usual Simpson's rule does with 500.

The coefficients of a five term polynomial approximation to each K are determined by the method of least squares. This gives

$$\begin{aligned} K_0(r) &= p_c + \sum_{n=1}^5 A_{1n} r^n \\ K_{2m}(r) &= \sum_{n=1}^5 A_{m+1,n} r^n, \quad m \geq 1 \end{aligned} \quad (3.56)$$

where A_{mn} , $m=1, 2, \dots, 40$; $n=1, 2, \dots, 5$ are known constants and $p_c = p(0, \theta)$. The polynomial form of the K's enable $g_m(t)$ to be determined also in polynomial form as in equation (3.24),

$$g_0(t) = p_c + \sum_{n=1}^5 c_{1n} t^n$$

$$g_{2m}(t) = \sum_{n=1}^5 c_{m+1,n} t^n, \quad m \geq 1 \quad (3.57)$$

where c_{mn} is given by equations (3.25) and (3.26).

The stress intensity factor may be obtained simply from equations (3.19) and (3.57). The integrals of equation (3.10) which give $D_m(\xi)$ may be evaluated in closed form in terms of spherical Bessel functions and the sine integral function. Recurrence relations between the integrals are used for the numerical calculations. The details are lengthy but straightforward. Finally, the integrals in eq.(3.22) involving $D_m(\xi)$ must be evaluated to obtain the function $q(y,z)$ of equation (3.22) which gives the nonsingular part of $\sigma_x(0,x,z)/p_0$. These integrals are evaluated by Simpson's rule using intervals of length 0.25 and integrating over segments of length 5.0 until the integral over the last segment is small compared to the total integral. As pointed out in the first part of this section, $q(y,z)$ is computed for various points of the yz -plane. The notation used for the results of this part of the numerical analysis is summarized in Table III.

Table III: Stress Intensity Factors and Stresses
on yz -Plane for Various Loads on Crack.

			$n \geq 1$
stress on crack $\sigma_z(x,y,0)/p_0 =$	eq. (3.51)/ p_0	$t^{(0)}(x,y) = -1$	$t^{(n)}(x,y)$
produces stress $\sigma_x(0,y,z)/p_0$ whose nonsing. part is =	$q_S(y,z)$	$q^{(0)}(y,z) =$ $\frac{2}{\pi} F_0(y,z)$ (see eq. (3.28))	$q_N^{(n)}(y,z)$
produces stress intensity factor $k_p(\theta)/\frac{2}{\pi} p_0 \sqrt{a} =$	$k_S(\theta)$	$k^{(0)}(\theta) = 1$	$k_N^{(n)}(\theta)$
For $n \geq 2$, $t^{(n)}(x,y) = \frac{4v}{\pi} k^{(n-2)}(\frac{\pi}{2}) t_S(x,y) + t_N^{(n)}(x,y)$ (See T.II)			
For $n \geq 1$, $k^{(n)}(\theta) = \frac{4v}{\pi} k^{(n-1)}(\frac{\pi}{2}) k_S(\theta) + k_N^{(n)}(\theta)$			

(3) Penny-shaped crack -- singular load

The singular stress on the crack was given in equation (3.39). For the numerical analysis consider the dimensionless form,

$$\sigma_z(x,y,0) = \frac{S(\psi_1)}{\sqrt{2R_1}} + \frac{S(\psi_2)}{\sqrt{2R_2}}$$

Note that since $\sigma_z > 0$, the singular part of the load on the crack gives a negative stress intensity factor. Further, since larger tensile stresses occur near the intersection of

the crack front with the surface, the stress intensity factor should be expected to be larger in magnitude there. Thus, when combined with the other contributions to the stress intensity factor, this will cause a decrease in the total as the surface is approached.

Because of the singularity, it would be advantageous to have a closed form solution for this part of the problem. But since none could be found, it was decided to use the same numerical method given for nonsingular loads. It is evident that more terms and finer mesh sizes are required. Limitations on computer time forced the use of the same number of points in r and the same number of terms in the r expansion as above. More terms were included in the Fourier series, and smaller subdivisions were used in the integration. It was found that $K_m(1)$ decreased very slowly as m increased. For $m=400$, $K_m(1)$ was of the order of 10^{-2} , $K_m(.967)$, of 10^{-3} , $K_m(.933)$, of 10^{-4} , and for $r < .5$, $K_m(r)$ was of the order 10^{-5} . For $m=1600$ these figures decreased by a factor of 10. Each time additional terms were included in the Fourier series, the magnitude of $k_S(\theta)$, the dimensionless stress intensity factor due to the singular pressure on the crack, increased near $\theta = \pi/2$ and remained the same elsewhere. Finally $k_S(\theta)$ was calculated using 841 terms in the cosine series.

The function $q_S(y, z)$ which gives the nonsingular part of the stress $\sigma_x(0, y, z)$ due to the load on the crack

was computed using 241 terms in the Fourier series. This part of the numerical solution required more than half of the computer time used. But note that the same function is used again in each iteration.

In reference [6] which also treats this problem there is no separation of singular and nonsingular terms in the numerical analysis. The half space problem utilizes stresses at points within Regions I and III of Figure 3.6. Outside these regions, the stress is approximated by zero. In [6], the stress is computed at 80 points within Region I, as compared with 45 in this analysis. The additional points should not be expected to account accurately for the singularities.

To obtain the stresses in the regions mentioned above and to obtain the stress intensity factor for a given stress on the penny shaped crack in [6], the stress on the crack is computed for five values of r and 19 values of θ . Weddle's rule is applied to the integrals for $K_m(r)$ for $m=0, 2, 4, \dots, 10$. Simpson's rule using, say, 40 values of θ should be as accurate. $K_m(r)$ is obtained in [6] as a fifth order polynomial in r by forcing the polynomial to pass through the computed points. In this work, $K_m(r)$ is known at 30 values of r , and the fifth-order polynomial is obtained by least squares curve fitting.

3.5 Discussion of Numerical Results

The result of the analysis described above is the curve in Figure 3.8 which shows the variation of the stress intensity factor along the crack front. The deepest point of the crack is $\theta=0$. Initially, moving away from this point, there is a gradual increase in stress intensity factor. Then about 20° from the surface there is a rapid increase. Following this a more rapid decrease occurs in the last 3° . Note that the stress intensity factor tends to zero at the surface, a result discussed in several previous papers [22, 28,29]. It appears that an increase in numerical accuracy would further decrease the value at the surface toward zero. However, the lack of an exact solution of the problem of a crack loaded by the stress of equation (3.51) is reflected by an accumulation of numerical inaccuracies as the number of iterations is increased.

Figure 3.8

It should be clear that the results in Figure 3.8 are by no means the exact solution of the problem but are presented as the best approximation available. The trend of the curves differs substantially from those obtained in [6] using basically the same numerical procedure. The results of [6], shown as a dashed line in Figure 3.8, would be expected to differ slightly from the present results because they were

obtained for a Poisson's ratio of 0.25 and the present ones, 0.30. The apparent reason for the qualitative difference between the results is the differing treatments of the singularities. As background information some intermediate results will be given.

The curve of Figure 3.8 is the result after the fourth iteration. The stress intensity factors after each iteration are shown in Figure 3.9. Each new iteration raises the stress intensity factor, but the amount of increase decreases as the number of iterations increases, with one exception. Near the surface the curve for the second iteration lies below that for the first.

As described in Section 3.3, the contribution of each iteration to the stress intensity factor consists of two parts. The two contributions for the first iteration are shown in Figure 3.10. The function $k_s(\theta)$ is used with each iteration as the stress intensity factor for the singular pressure on the crack. The curve for $k_N^{(1)}(\theta)$ comes from the nonsingular part of the stress being removed from the crack by this iteration. The combination of the two designated $k^{(1)}(\theta)$ is what this iteration adds to the previous total stress intensity factor. (In this case, $k(\theta) = k^{(0)}(\theta) = 1$.)

Figure 3.9

Figure 3.10

4. FUTURE APPLICATIONS - SEMI-ELLIPTICAL CRACK

The problem of a flat elliptical crack lying completely within a half space and perpendicular to the surface has already been attempted in [9]. The results in [9] for the case in which the major axis of the ellipse lies in the surface (Figure 4.1) are labeled as approximate in recognition of the greater accuracy required due to the intersection of the crack front with the surface. The troublesome singularities encountered in the alternating method which were discussed in detail in Section 3.4 are present in the semi-elliptical surface crack problem. Such considerations are neglected in [9], but other difficulties remain. The major difficulty is that the solution for the elliptical crack in an infinite medium is extremely complicated.

Figure 4.1

For the penny-shaped crack problem, the pressure on the crack needs only to permit a cosine series expansion of the form of equations (3.23) and (3.30). And the inclusion of more terms in the series is easily handled because of the nature of the solution. However, the solution for the elliptical crack requires the pressure to be given as a polynomial

$$p(x,y) = \sum_{n=0}^N \sum_{m=0}^M a_{mn} x^m y^n \quad (4.1)$$

It is possible to work out the solution for any finite number of terms of equation (4.1), although, for a large number, it is impractical. Thus far, no way has been found to include the effect of additional terms in (4.1) by a recurrence scheme. The additional terms require the solution for the lower order terms and additional contributions combined in a complicated way.

As a result of the difficulty, the elliptical crack problem was restricted in [9] to be of the form

$$p(x,y) = a_{00} + a_{01}y + a_{20}x^2 + a_{02}y^2 + a_{21}x^2y + a_{03}y^3 \quad (4.2)$$

The six constants in this equation are determined by a least squares technique of fitting equation (4.2) to a number of known values of $p(x,y)$. The odd powers of x are omitted because the problem is taken to be symmetric about the yz -plane. For the elliptical surface flaw, the pressure would also be made symmetric about the xz -plane, and the odd powers of y would be eliminated. Thus, only three constants, a_{00} , a_{20} , a_{02} , would be available for the least square fitting necessary. Additional terms are clearly needed, but the 200 terms used in the penny-shaped crack solution (40 in θ , 5 in r) cannot be approached.

As suggested by Kantorovich and Krylov [2], the Schwarz-Neumann Alternating Technique has wide applicability. It can be applied to other three-dimensional crack problems of interest such as the finite thickness crack problem. The crack may be taken to intersect the plate at any angle. Such problems would involve combined modes of crack extension even though the plate is loaded in simple tension.

There is some arbitrariness in the choice of the two sequences of problems involved in the alternating method. For example, in Section 2.3, the stress, $\sigma(x)$, on the edge crack was extended symmetrically to negative values of x in the zeroth iteration. It would have been possible to make the stress skew-symmetric about the y -axis instead. The two sequences of problems would then be quite different. Similarly, in the surface crack problem, the initial pressure on the penny-shaped crack could be taken to be skew-symmetric about the yz -plane. The problems which make up the two sequences would then have different characteristics. In general, the various alternatives should be studied to determine whether one provides a better representation of the essential properties of the problem.

It is conceivable that in some applications the alternating method will involve three or more sequences of solutions. In general, one sequence would be expected to be necessary for each part of the boundary of the material.

If there were three parts of the boundary and three solutions, the sequence would be formed similarly to the examples presented here. Each solution would produce some undesirable residual stresses on the other two boundaries. Thus, each iteration would use each solution in turn to remove the residual stresses produced by the other two solutions in their previous applications.

APPENDIX

Stress intensity factors for various particular loads on the edge crack are listed here. For other loads the general expression of eq.(2.50) may be used. In addition, results for the penny-shaped crack in an infinite body are given, includigg some recently published stress intensity factors for non-axisymmetrically loaded cracks.

Edge Cracks

(1) Concentrated forces (Figure 2.4)

For concentrated normal and shearing forces applied to the crack as shown in Figure 2.4, the stress intensity factors are

$$k_1 = \frac{2}{\pi} P \sqrt{a} \frac{1+f(b/a)}{\sqrt{a^2-b^2}}$$

$$k_2 = \frac{2}{\pi} Q \sqrt{a} \frac{1+f(b/a)}{\sqrt{a^2-b^2}}$$

where $f(b/a)$ is given by equation (2.47) and Figure 2.5.

Figure A-1

(2) Linear stress (Figure A-1)

In this case, the stress on the crack varies linearly from zero at the edge to twice the average stress at the crack tip (Figure A-1). The stress intensity factors in

terms of the average stresses are

$$k_1 = 1.3660 \sigma_a \sqrt{a}$$

$$k_2 = 1.3660 \tau_a \sqrt{a}$$

Figure A-2

(3) Uniform stress near crack tip (Figure A-2)

As shown in Figure A-2, the crack is free of stress on the part of its faces adjacent to the edge and is subjected to uniform stresses on the other part up to the crack tip. The stress intensity factors may be expressed as

$$k_1 = \frac{2}{\pi} \arccos(b/a) \sigma_0 \sqrt{a} [1 + h_1(b/a)]$$

$$k_2 = \frac{2}{\pi} \arccos(b/a) \tau_0 \sqrt{a} [1 + h_1(b/a)]$$

where $h_1(b/a)$ is shown in Figure A-3. These results may also be expressed in terms of the average stresses on the crack,

$$\sigma_a = (1 - b/a) \sigma_0 \quad \tau_a = (1 - b/a) \tau_0$$

The stress intensity factors

$$k_1 = h_2(b/a) \sigma_a \sqrt{a}$$

$$k_2 = h_2(b/a) \tau_a \sqrt{a}$$

then show the expected increase when the same total load is applied nearer the crack tip. See Figure A-3.

Figure A-3

(4) Uniform stress (See Table I)

In the case of uniform shear loading, the stress where the crack intersects the edge must be zero. See also the discussion in Section 2.4 of a similar restriction on the normal stress when the alternating method is used directly. These restrictions do not affect the use of case (3) above for very small values of b/a . As $b/a \rightarrow 0$ it is found that

$$k_1 = 1.1215 \sigma_0 \sqrt{a}$$

$$k_2 = 1.1215 \tau_0 \sqrt{a}$$

By superposition the first result may be applied to the case of uniform tension at infinity parallel to the free edge when the crack is stress free. There is no corresponding application of the second result.

(5) Polynomial stress [18]

If the form of the stress in Figure A-1 is not linear, but is given by

$$\sigma_y(x,0) = -\sigma_0 \sum_{n=0}^{10} c_n (x/a)^n$$

where C_0, C_1, \dots, C_{10} are arbitrary constants, then the stress intensity factor is [18]

$$k_1 = \sigma_0 \sqrt{2a} [0.7930C_0 + 0.4829C_1 + 0.3716C_2 + 0.3118C_3 + 0.2735C_4 + 0.2464C_5 + 0.2260C_6 + 0.2099C_7 + 0.1968C_8 + 0.1858C_9 + 0.1765C_{10}]$$

If there is shear loading $\tau_{xy}(x,0)$ given by the expression for $\sigma_y(x,0)$, but with σ_0 replaced by τ_0 , then by the statement following eq.(2.50), the Mode II stress intensity factor, k_2 , is given by the expression for k_1 with σ_0 replaced by τ_0 .

Penny-Shaped Cracks

(6) General result (Figure 3.1)

The pressure applied to the crack is in the form

$$\sigma_z = -p_0 \sum_{m=0}^{\infty} K_m(r) \cos m\theta, \quad z=0, \quad r \leq 1$$

where r is the distance from the z -axis divided by the crack radius, a . The resulting Mode I stress intensity factor is

$$k_1 = \frac{2}{\pi} p_0 \sqrt{a} \sum_{m=0}^{\infty} g_m(1) \cos m\theta$$

where

$$g_m(t) = \int_0^1 K_m(t\zeta) \frac{\zeta^{m+1} d\zeta}{\sqrt{1-\zeta^2}}$$

These formulas apply only when the stress on the crack is symmetric about a plane containing the z-axis (the $\theta=0$ plane). For the special case of axisymmetric loading the only nonzero $K_m(r)$ is $K_0(r)$, and the equations simplify considerably.

(7) Uniform tension (Figure A-4) [26]

By superposition, the stress intensity factor due to the uniaxial tension may be determined by considering the same geometry, but with uniform pressure,

$$\sigma_z = -\sigma_0, \quad z=0, \quad r < 1$$

on the crack and zero stress at infinity. For this problem the parameters of case (6) are

$$p_0 = \sigma_0, \quad K_0(r) = 1, \quad K_m(r) = 0, \quad m \geq 1$$

Therefore, the stress intensity factor is [26].

$$k_1 = \frac{2}{\pi} \sigma_0 \sqrt{a}$$

Figure A-4

(8) Uniform shear (Figure A-4) [30]

The solution in [30] for constant shearing stresses on the faces of a penny-shaped crack may be used to obtain the stress intensity factors for Figure A-4.

$$k_2 = \frac{1}{2-\nu} \frac{4}{\pi} \tau_0 \sqrt{a} \sin\theta$$

$$k_3 = \frac{1-\nu}{2-\nu} \frac{4}{\pi} \tau_0 \sqrt{a} \cos\theta$$

The uniform shear load produces no Mode I stress intensity factor.

Figure A-5

(9) Concentrated forces (Figure A-5) [6]

The stress intensity factors for Modes II and III are zero, and

$$k_1 = \frac{2}{\pi} \frac{2P}{\pi a^2} \sqrt{a} \frac{1}{\sqrt{1-r^2}} \left[\frac{1}{2} + \sum_{m=1}^{\infty} r_1^m \cos m\theta_1 \cos m\theta \right]$$

The two pairs of concentrated forces act a distance of ar_1 out on the rays $\theta = \pm\theta_1$.

In the case of a single pair of forces of magnitude F on the crack, θ_1 may be put equal to zero and $2P$ replaced by F in the above expression. If, further, the single pair of forces acts at the center of the crack,

$$k_1 = \frac{1}{\pi} \frac{F}{\pi a^2} \sqrt{a}$$

(10) Linear stress [6]

Case (6) may be applied to the case of normal stress varying linearly with $x=r\cos\theta$. For

$$\sigma_{zz} = -p_0 r \cos\theta, \quad z = 0, \quad r < 1$$

the stress varies from zero on the y-axis to a maximum of p_0 at the points where the crack front intersects the x-axis of Figure 3.1. The only non-zero $K_m(r)$ is

$$K_1(r) = r$$

and the stress intensity factor,

$$k_1 = \frac{4}{3\pi} p_0 \sqrt{a} \cos\theta$$

is easily obtained.

Figure A-6

(11) Bending stress (Figure A-6)[6]

Cases (7) and (10) may be superposed to obtain the solution of the bending of a beam containing a small penny-shaped crack in a transverse section. If the crack is far enough from the lateral surfaces of the beam their interaction may be neglected. Reference [6] specifies

$$d > 3a$$

$$c-b > 3a$$

where the dimensions of the beam are shown in Figure A-6. An additional restriction must be placed on the dimensions to insure that the crack faces are not compressed together, for the solution would be invalid if that happened. This restriction,

$$b > \frac{2}{3} a$$

simply makes the stress intensity factor positive at all points of the crack front. In terms of the moment of inertia, $I = 2dc^3/3$, of the cross-section, the stress produced in an uncracked beam is

$$\sigma_{zz} = \frac{M_0 a}{I} (b/a - r\cos\theta), \quad z = 0, \quad r < 1$$

By superposition, the stress intensity factor

$$k_1 = \frac{2}{\pi} \frac{M_0 a}{I} \sqrt{a} (b/a - (2/3)\cos\theta)$$

may be found by considering the beam to be loaded only by stresses on the faces of the crack equal and opposite to those produced in the uncracked beam.

Surface Crack

(12) Uniform stress

The geometry of the half penny-shaped crack at the surface of a half space is shown in Figure 3.6. For the case of uniform tension at infinity perpendicular to the crack (or uniform pressure on the crack faces), the stress intensity factor is given in Figure 3.8.

REFERENCES

- [1] Paris, P. C. and Sih, G. C., "Stress Analysis of Cracks", Fracture Toughness Testing and Its Applications, ASTM STP 381, 1965, pp. 30-83.
- [2] Kantorovich, L. V. and Krylov, V. I., Approximate Methods of Higher Analysis, Interscience, New York, 1964.
- [3] Irwin, G. R., "The Crack-Extension Force for a Crack at a Free Surface Boundary", U.S. Naval Research Lab. Rept. 5120, 1958.
- [4] Lachenbruch, A. H., "Depth and Spacing of Tension Cracks", J. Geophys. Res., Vol. 66 (1961), pp. 4273-4292.
- [5] Brož, P., "On the Solution of an Infinite Strip Weakened by a Transverse Crack", Acta Technica Čsav, Vol. 15 (1970), pp. 724-760.
- [6] Smith, F. W., Kobayashi, A. S., Emery, A. F., "Stress Intensity Factors for Penny-Shaped Cracks, Part 1 - Infinite Solid" and "Stress Intensity Factors for Semicircular Cracks, Part 2 - Semi-Infinite Solid", J. Appl. Mech., Vol. 34 (1967), pp. 947-959.
- [7] Smith, F. W. and Alavi, M. J., "Stress-Intensity Factors for a Part-Circular Surface Flaw", Proc. First Int. Conf. Pres. Ves. Tech., Delft, The Netherlands, 1969.
- [8] Smith, F. W. and Alavi, M. J., "Stress Intensity Factors for a Penny Shaped Crack in a Half Space", Engr. Fract. Mech. to be published.
- [9] Shah, R. C., and Kobayashi, A. S., "Stress Intensity Factors for an Elliptical Crack Approaching the Surface of a Semi-Infinite Solid", Int. J. Fract. Mech. (in press).
- [10] Irwin, G. R., "Crack Extension Force for a Part-Through Crack in a Plate", J. Appl. Mech., Vol. 29 (1962), pp. 651-654.
- [11] Bueckner, H. F., "Some Stress Singularities and Their Computation by Means of Integral Equations", Boundary Problems in Differential Equations, University of Wisconsin Press, Madison, Wis., 1960.

- [12] Winne, D.H. and Wundt, B.M., "Application of the Griffith-Irwin Theory of Crack Propagation to the Bursting Behavior of Disks, Including Analytical and Experimental Studies", Trans. ASME, Vol. 80 (1958), pp. 1643-1655.
- [13] Koiter, W.T., discussion of paper by Bowie, J. Appl. Mech., Vol. 32 (1965), p. 237.
- [14] Koiter, W.T., "On the Flexural Rigidity of a Beam Weakened by Transverse Saw-Cuts", Proc. Kon. Ned. Akad. Wet. (B), Vol. 59 (1956), pp. 354-374.
- [15] Sneddon, I.N., Fourier Transforms, McGraw-Hill, New York, 1951.
- [16] Wigglesworth, L.A., "Stress Distribution in a Notched Plate", Mathematika, Vol. 4 (1957), pp. 76-96.
- [17] Doran, H.E. and Buchwald, V.T., "The Half-Plane with an Edge Crack in Plane Elastostatics", J. Inst. Maths. Applics., Vol. 5 (1969), pp. 91-112.
- [18] Stallybrass, M.P., "A Crack Perpendicular to an Elastic Half-Plane", Int. J. Engr. Sci., Vol. 8 (1970), pp. 351-362.
- [19] Sneddon, I.N. and Das, S.C., "The Stress Intensity Factor at the Tip of an Edge Crack in an Elastic Half Plane", Int. J. Engr. Sci., Vol. 9 (1971), pp. 25-36.
- [20] Magnus, W. and Oberhettinger, F., Formulas and Theorems for the Functions of Mathematical Physics, Chelsea, New York, 1949.
- [21] Sih, G.C. and Liebowitz, H., "Mathematical Theories of Brittle Fracture", Fracture, Vol. 2, Academic Press, New York, 1968.
- [22] Sih, G.C., "A Review of the Three-Dimensional Stress Problem for a Cracked Plate", Int. J. Fract. Mech., Vol. 7 (1971), pp. 39-61.
- [23] Thresher, R.W. and Smith, F.W., "Stress Intensity Factors for a Surface Crack in a Finite Solid" ASME Paper No. 71-APMW-6, J. Appl. Mech., in press.
- [24] Muki, R., "Asymmetric Problems of the Theory of Elasticity for a Semi-Infinite Solid and a Thick Plate", Progress in Solid Mechanics, Vol. 1., North-Holland Publishing Co., Amsterdam, 1960, pp. 401-439.

- [25] Love, A.E.H., "The Stress Produced in a Semi-Infinite Solid by Pressure on Part of the Boundary", Phil. Trans. Roy. Soc. (A), Vol. 228 (1929), pp. 377-420.
- [26] Sneddon, I.N., "The Distribution of Stress in the Neighbourhood of a Crack in an Elastic Solid", Proc. Roy. Soc. (A), Vol. 187 (1946), pp. 229-260.
- [27] Filon, L.N.G., "On a Quadrature Formula for Trigonometric Integrals", Proc. Roy. Soc. Edin., Vol. 49 (1928-29), pp. 38-47.
- [28] Hartranft, R.J. and Sih, G.C., "The Use of Eigenfunction Expansions in the General Solution of Three-Dimensional Crack Problems", J. Math. Mech., Vol. 19 (1969), pp. 123-138.
- [29] Sih, G.C., Williams, M.L., Swedlow, J.L., "Three-Dimensional Stress Distribution Near a Sharp Crack in a Plate of Finite Thickness", Air Force Materials Laboratory, Wright-Patterson Air Force Base, November 1966 (AFML-TR-66-242).
- [30] Segedin, C.M., "Note on a Penny-Shaped Crack Under Shear", Proc. Camb. Phil. Soc., Vol. 47 (1951), pp. 396-400.

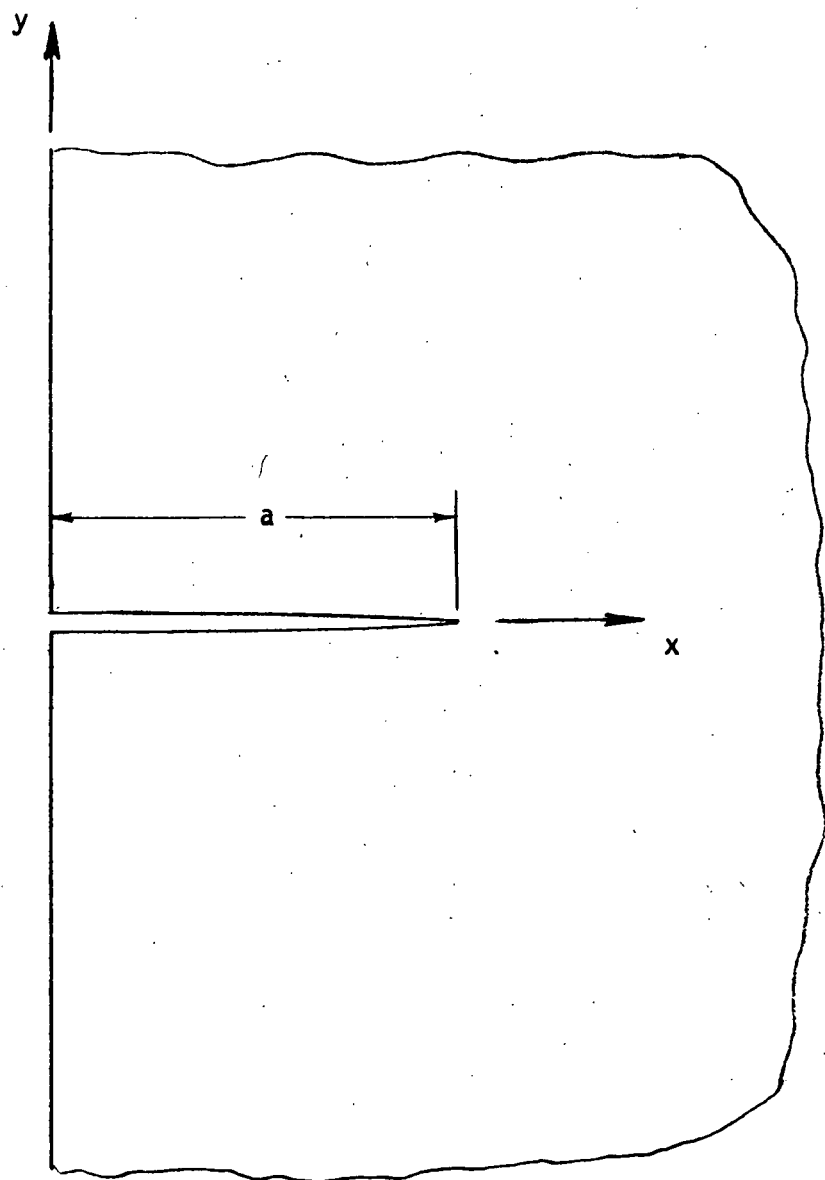


Fig. 2.1: Edge-cracked plate

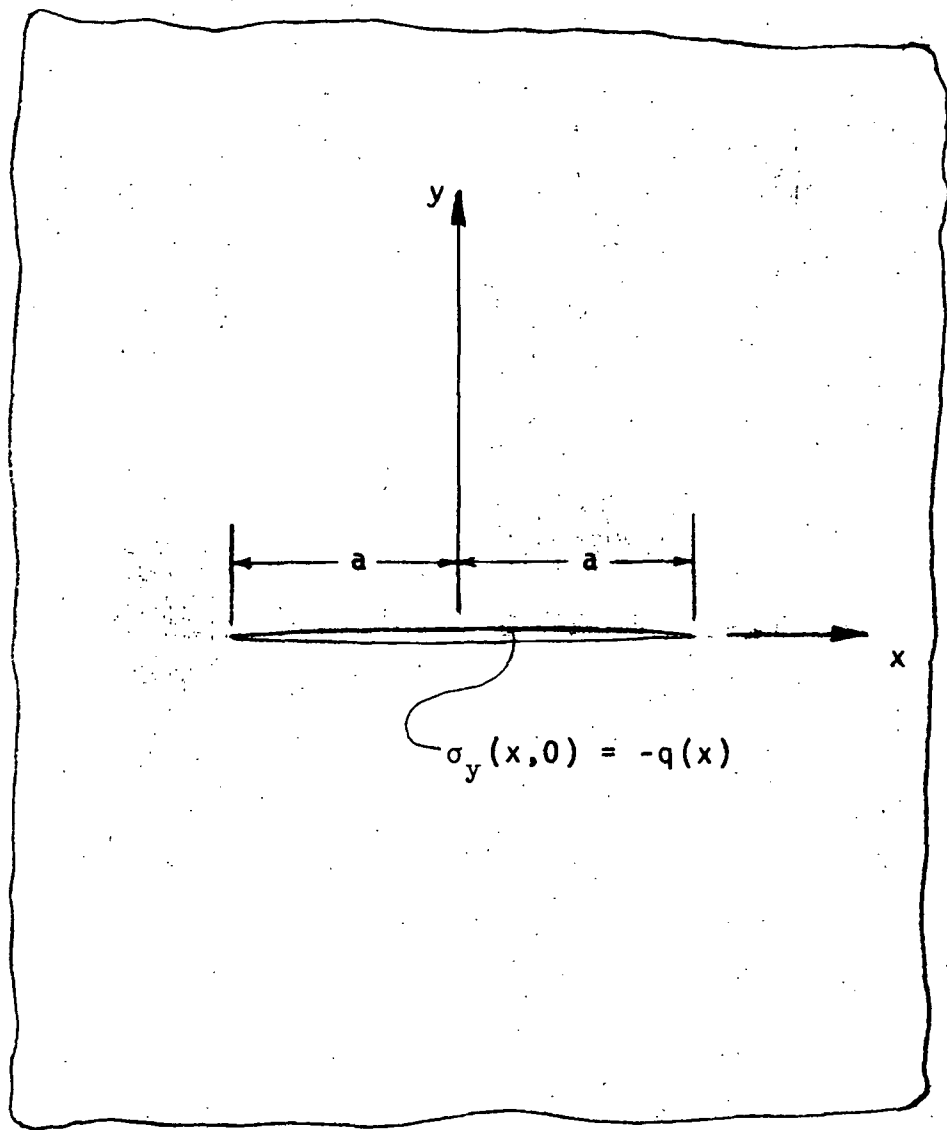


Fig. 2.2: Cracked infinite plate

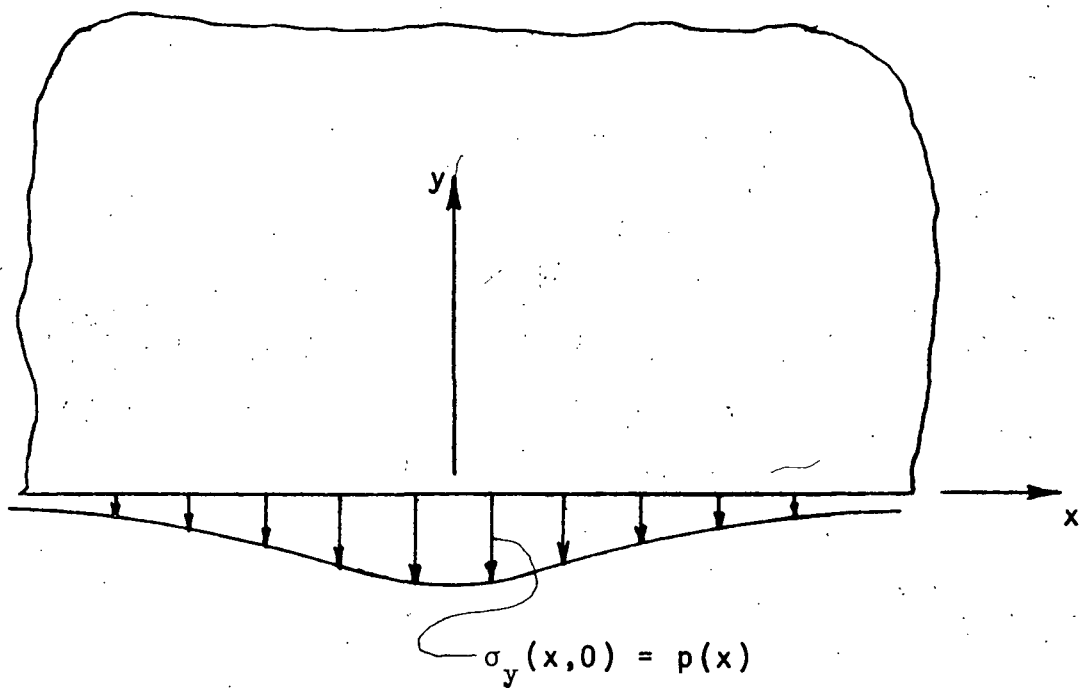


Fig. 2.3: Edge-loaded half plane

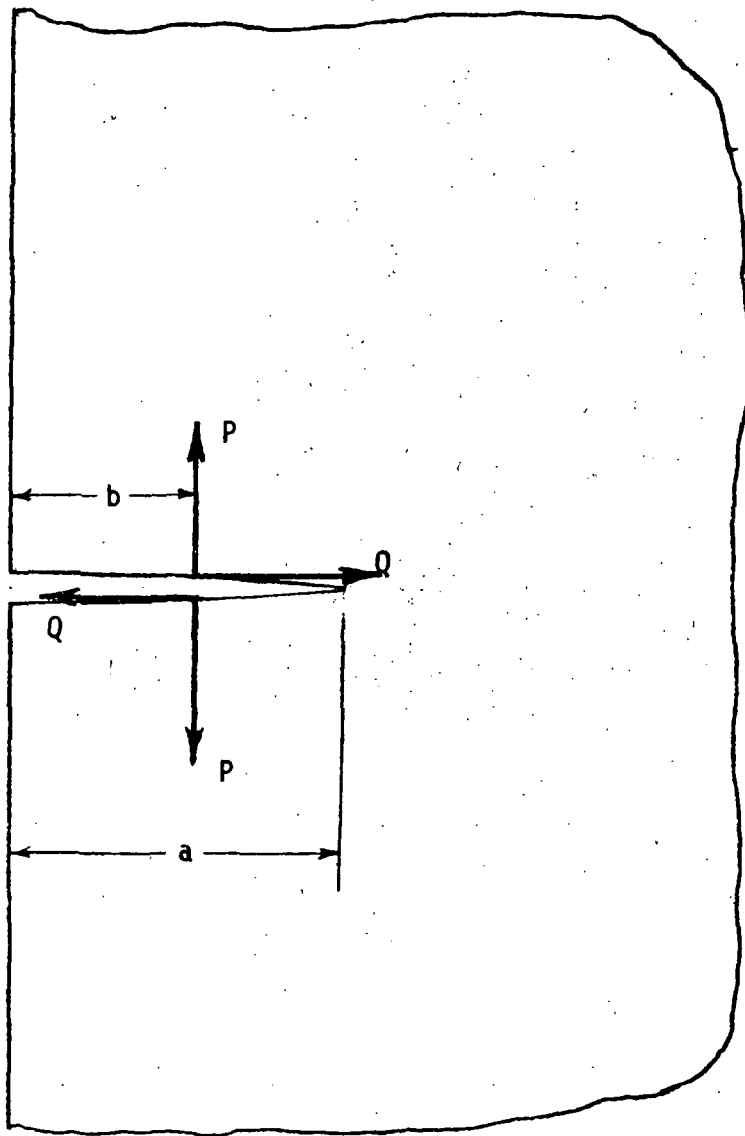


Fig. 2.4: Concentrated forces on an edge crack

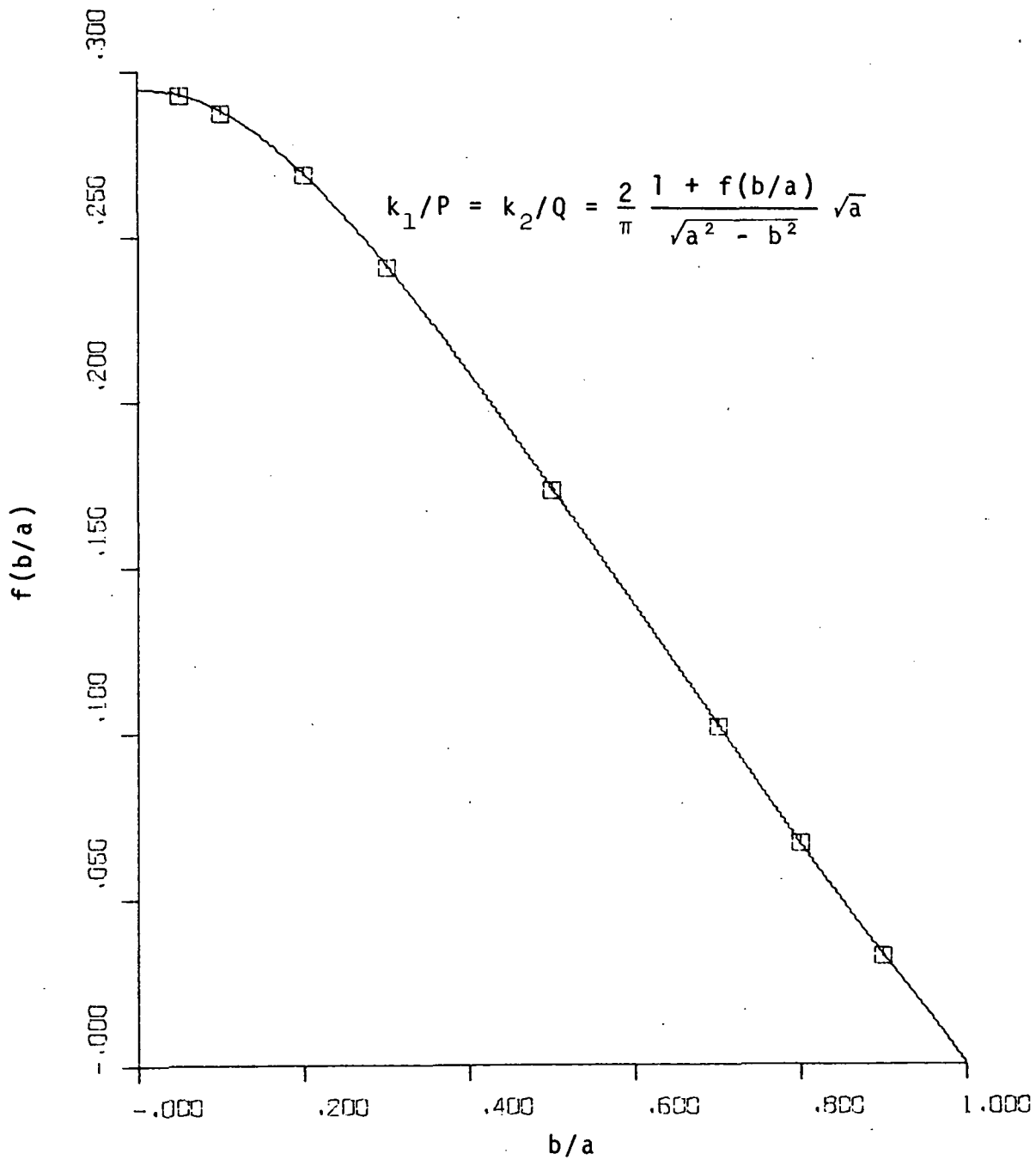


Fig. 2.5: Stress intensity factor correction for concentrated forces on an edge crack

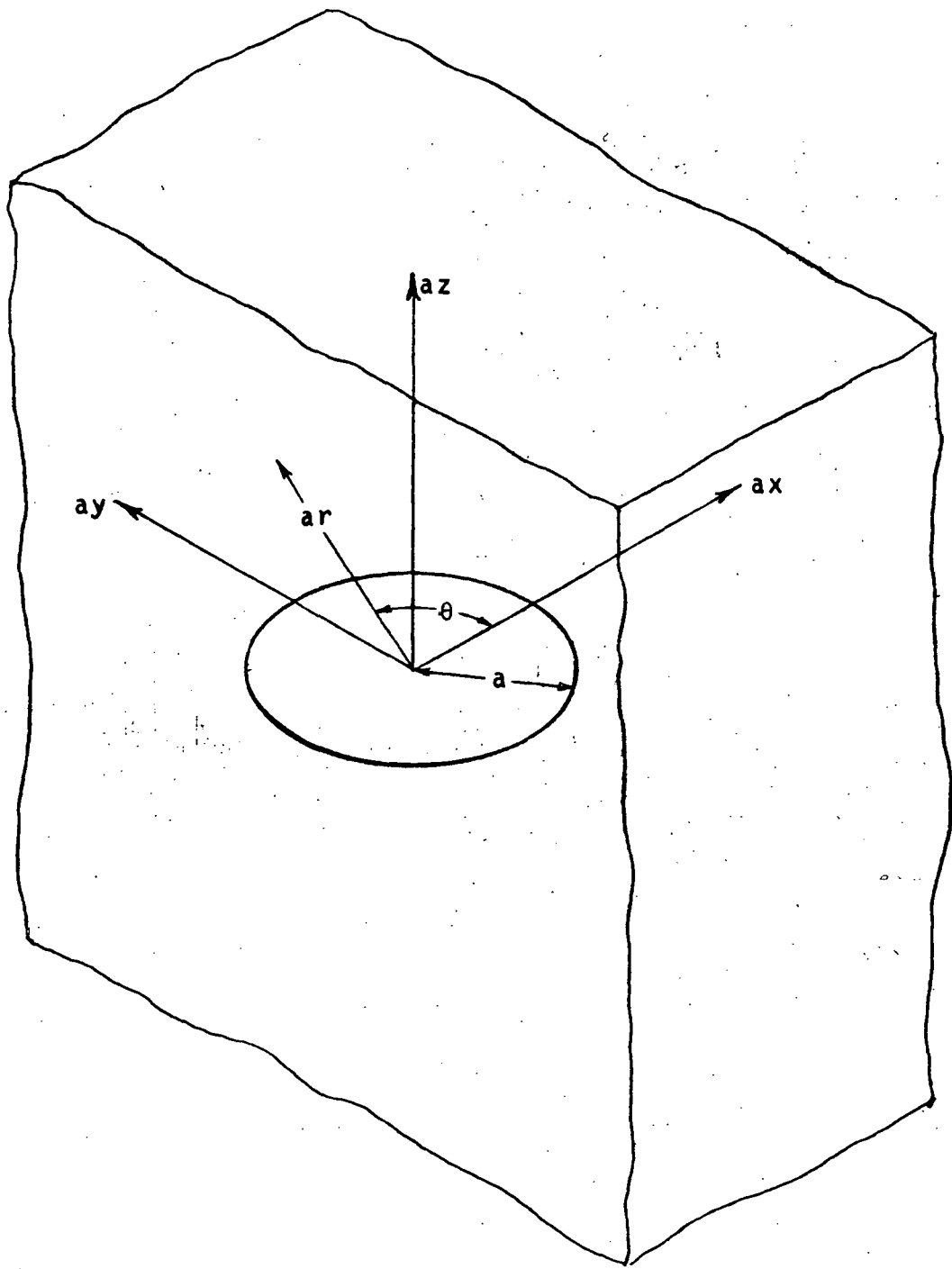


Fig. 3.1: Penny-shaped crack in infinite body

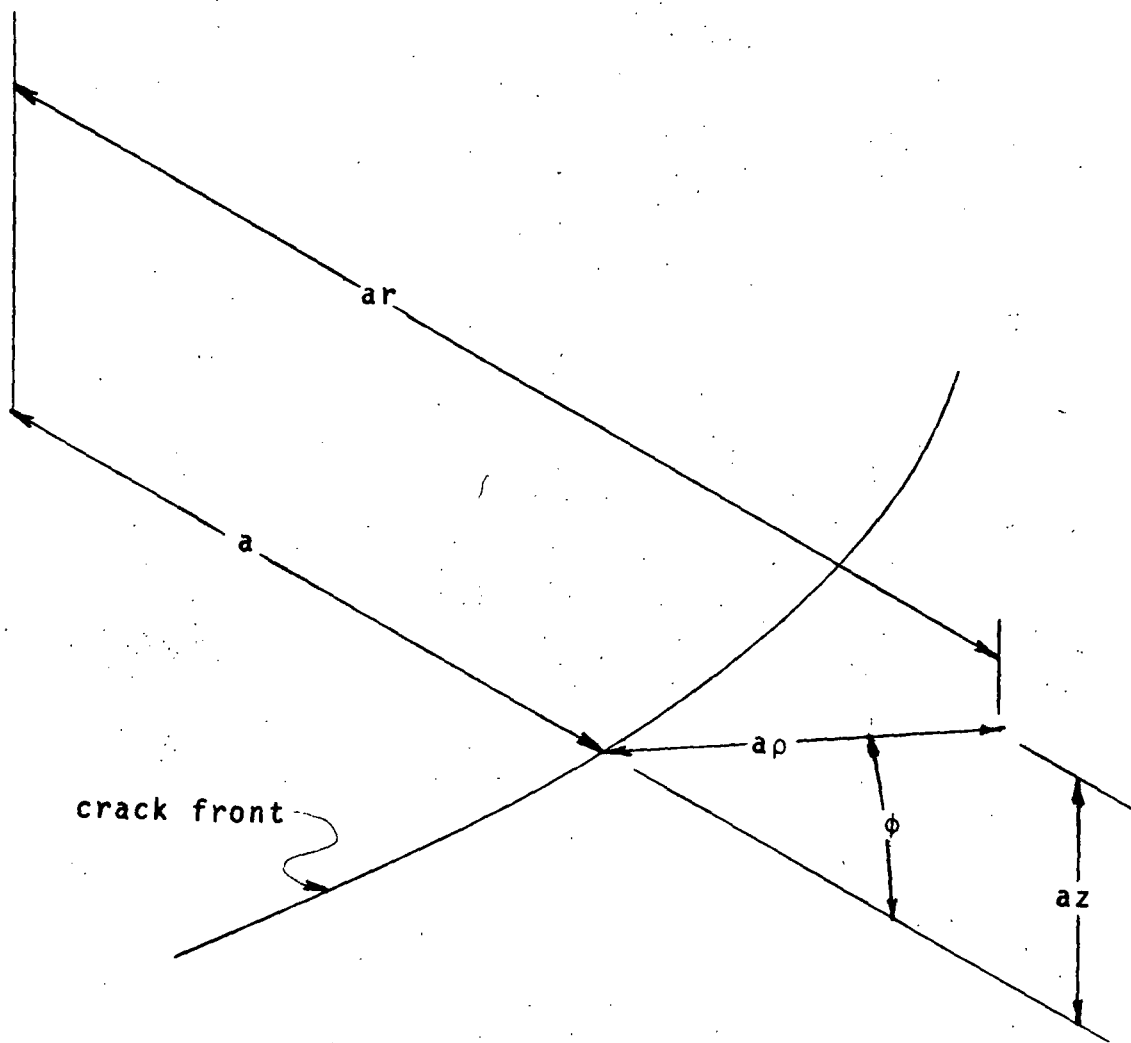


Fig. 3.2: Local coordinates (ρ, ϕ) at crack front

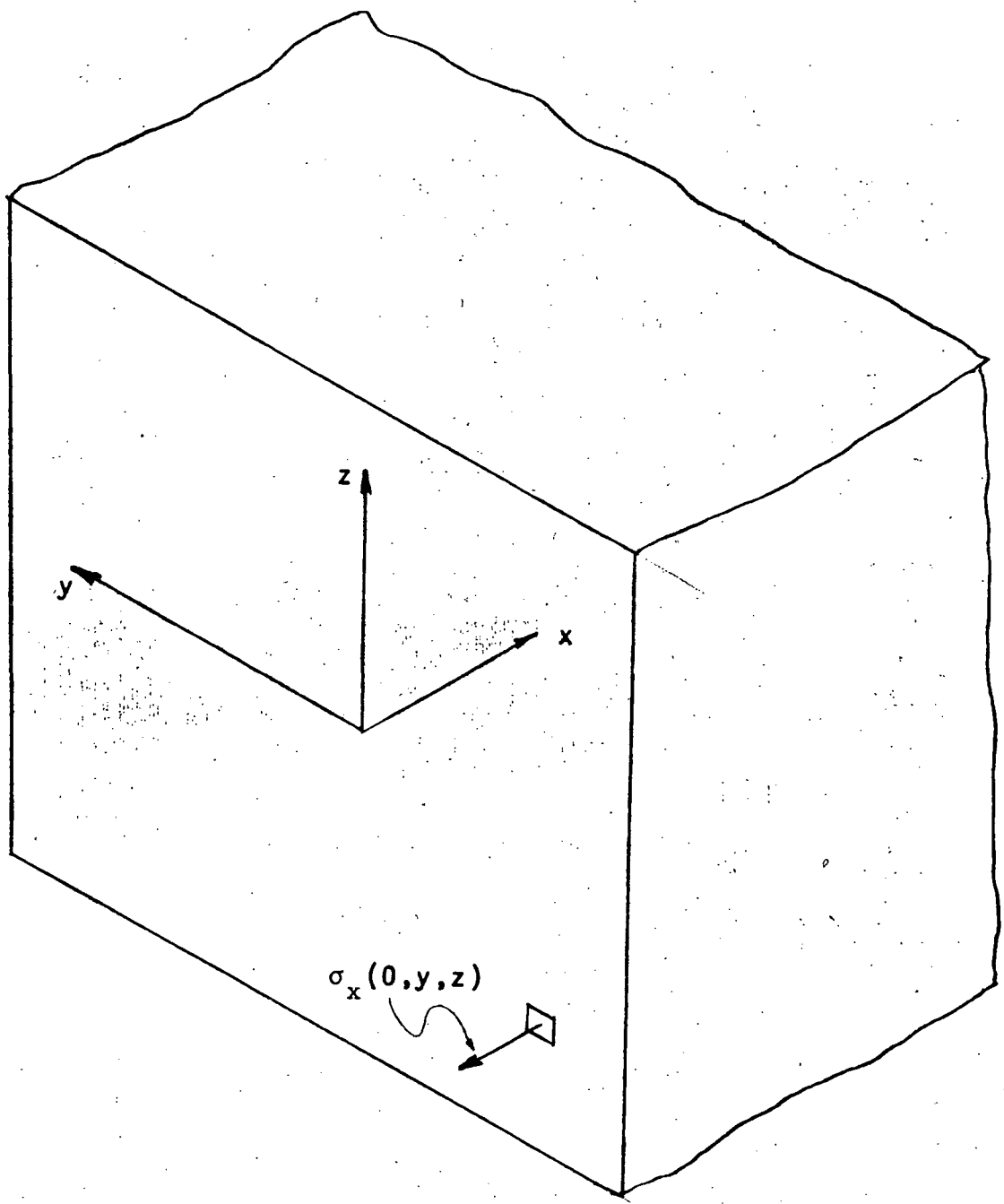


Fig. 3.3: Half space ($x \geq 0$) loaded on surface ($x = 0$)

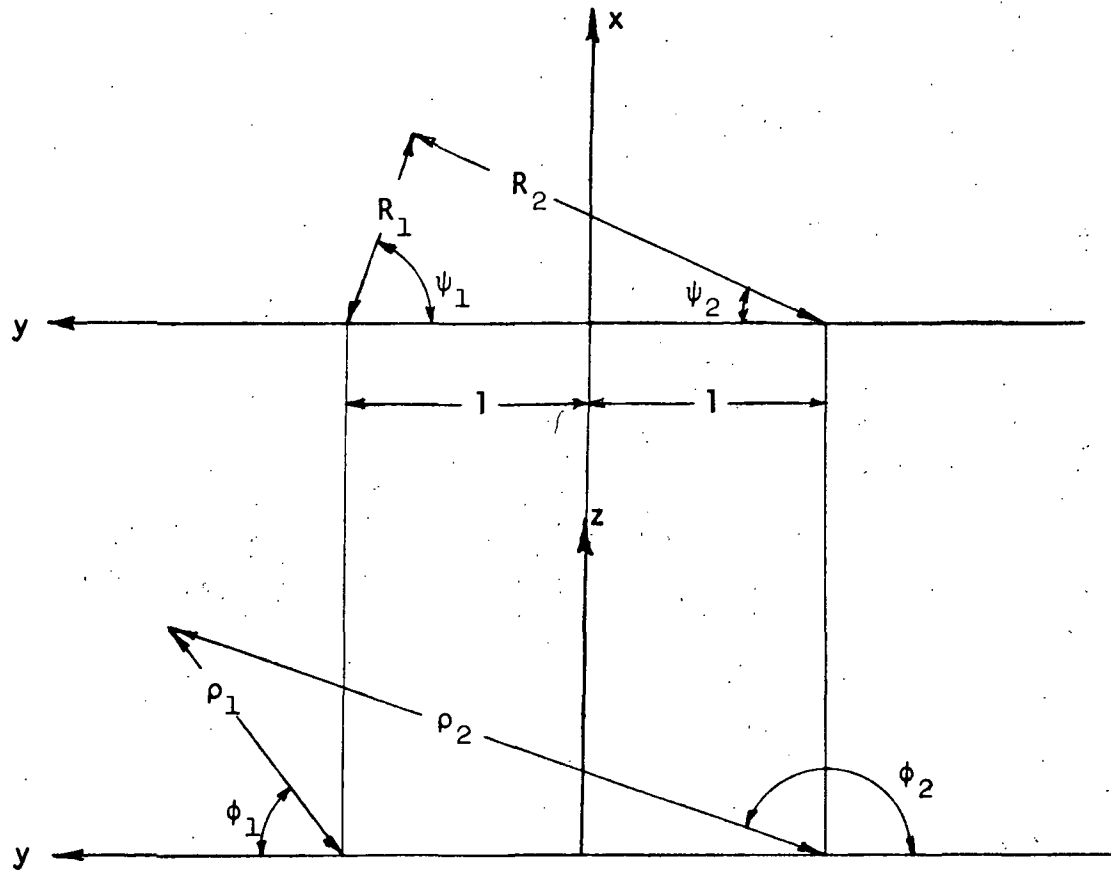


Fig. 3.4: Auxiliary coordinates for singular solutions

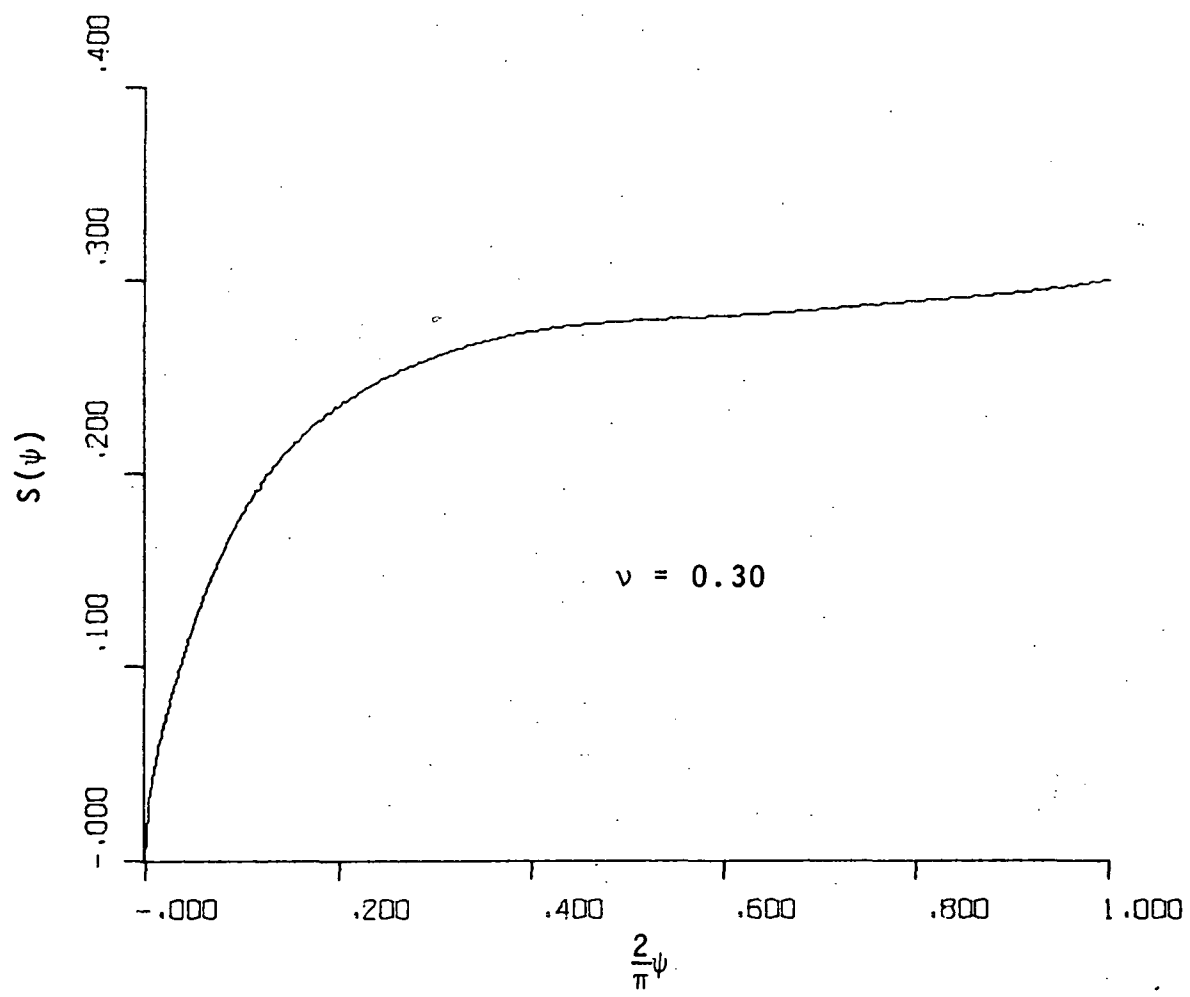


Fig. 3.5: Function for eq.(3.39) for singular normal stress on half space

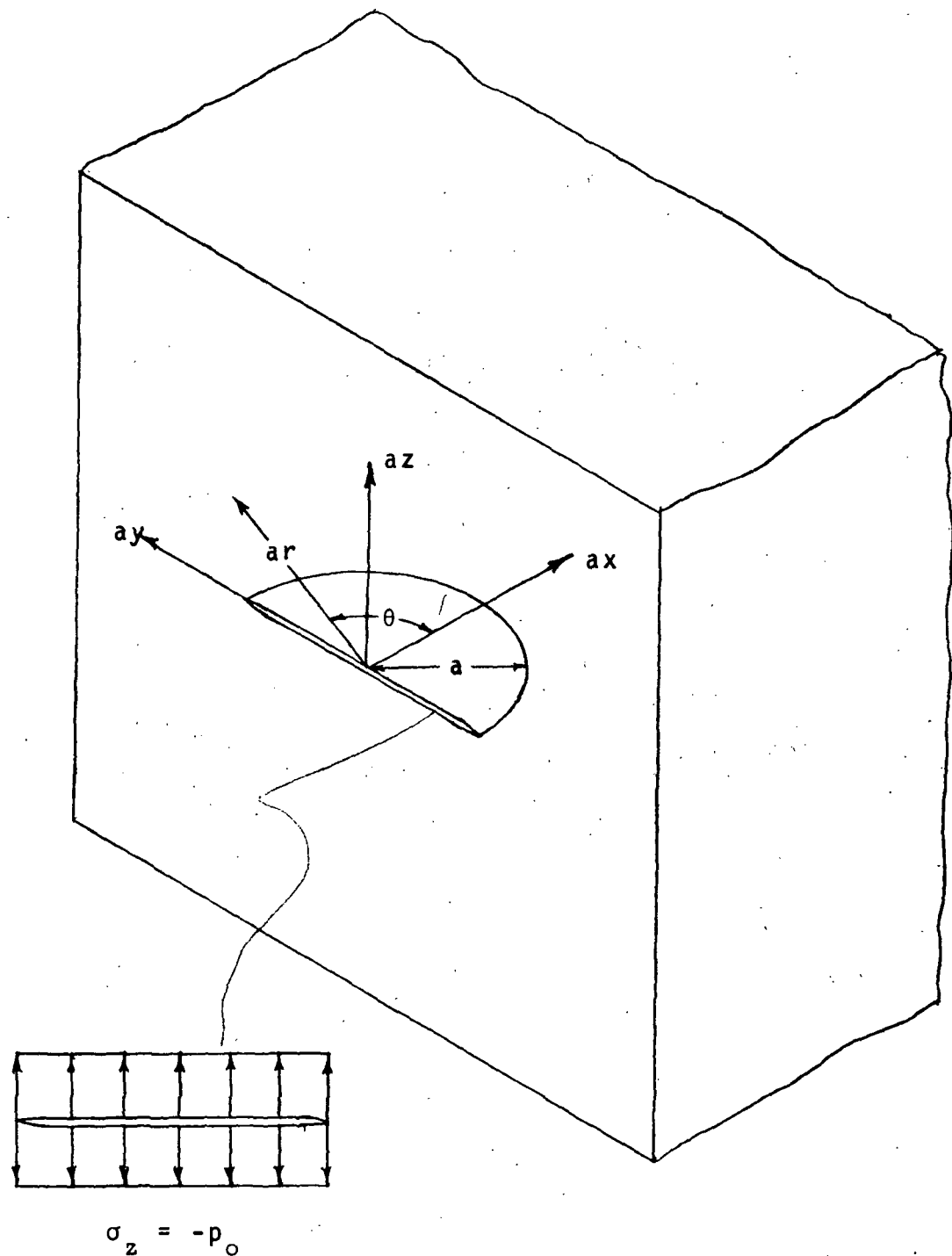


Fig. 3.6: Half penny surface crack

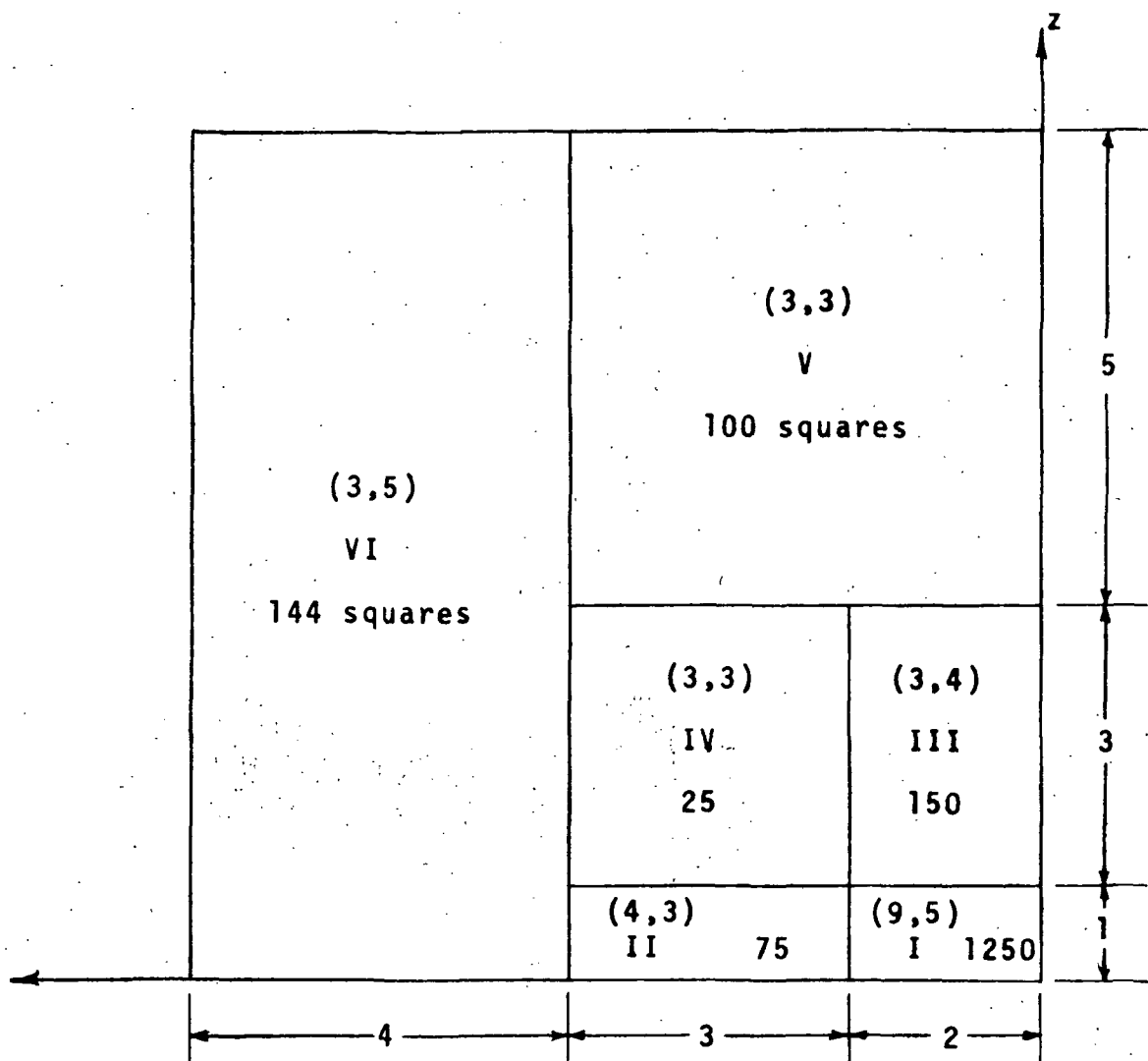


Fig. 3.7: Grid on surface of half space

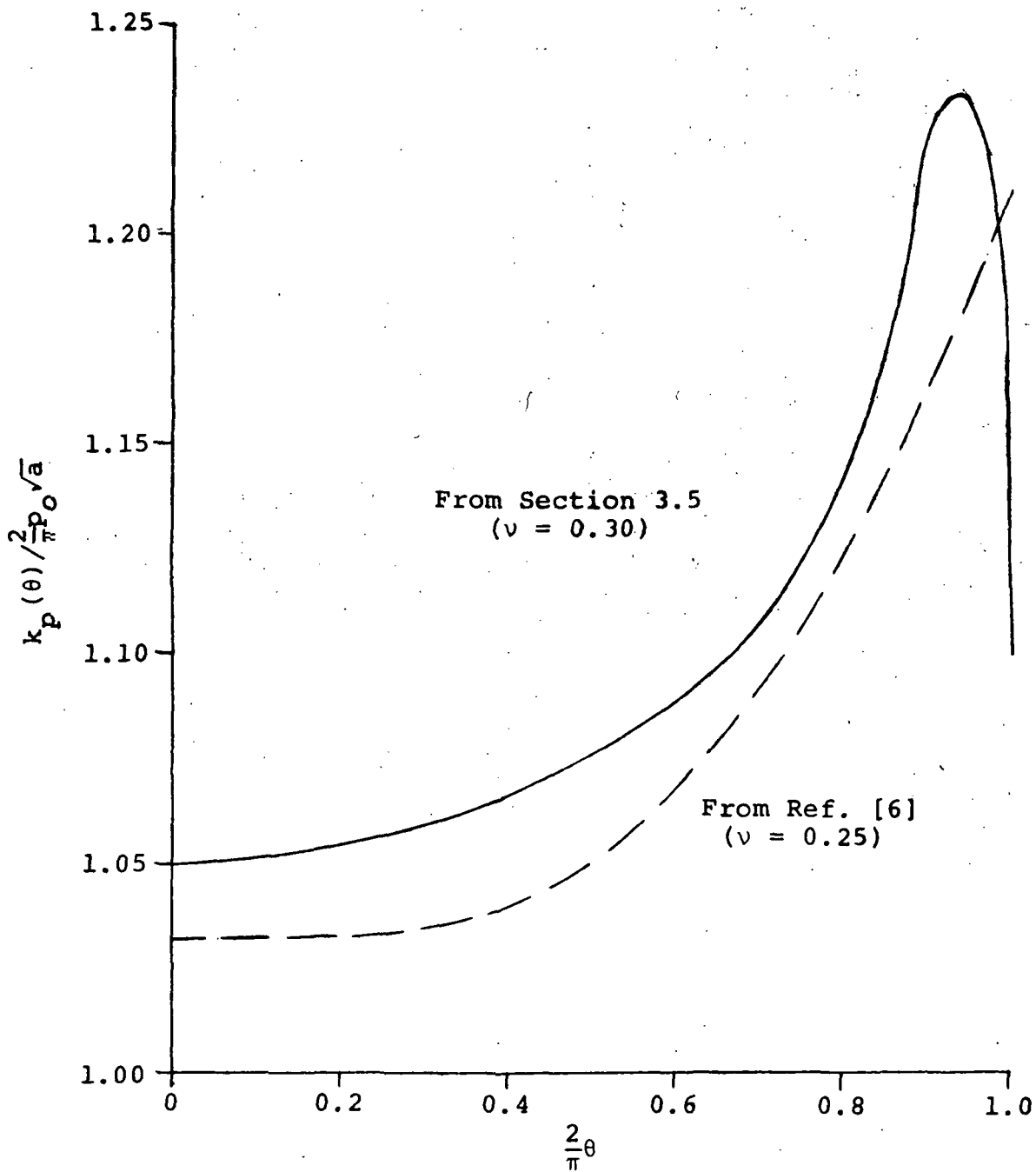


Fig. 3.8: Stress intensity factor for Fig. 3.6

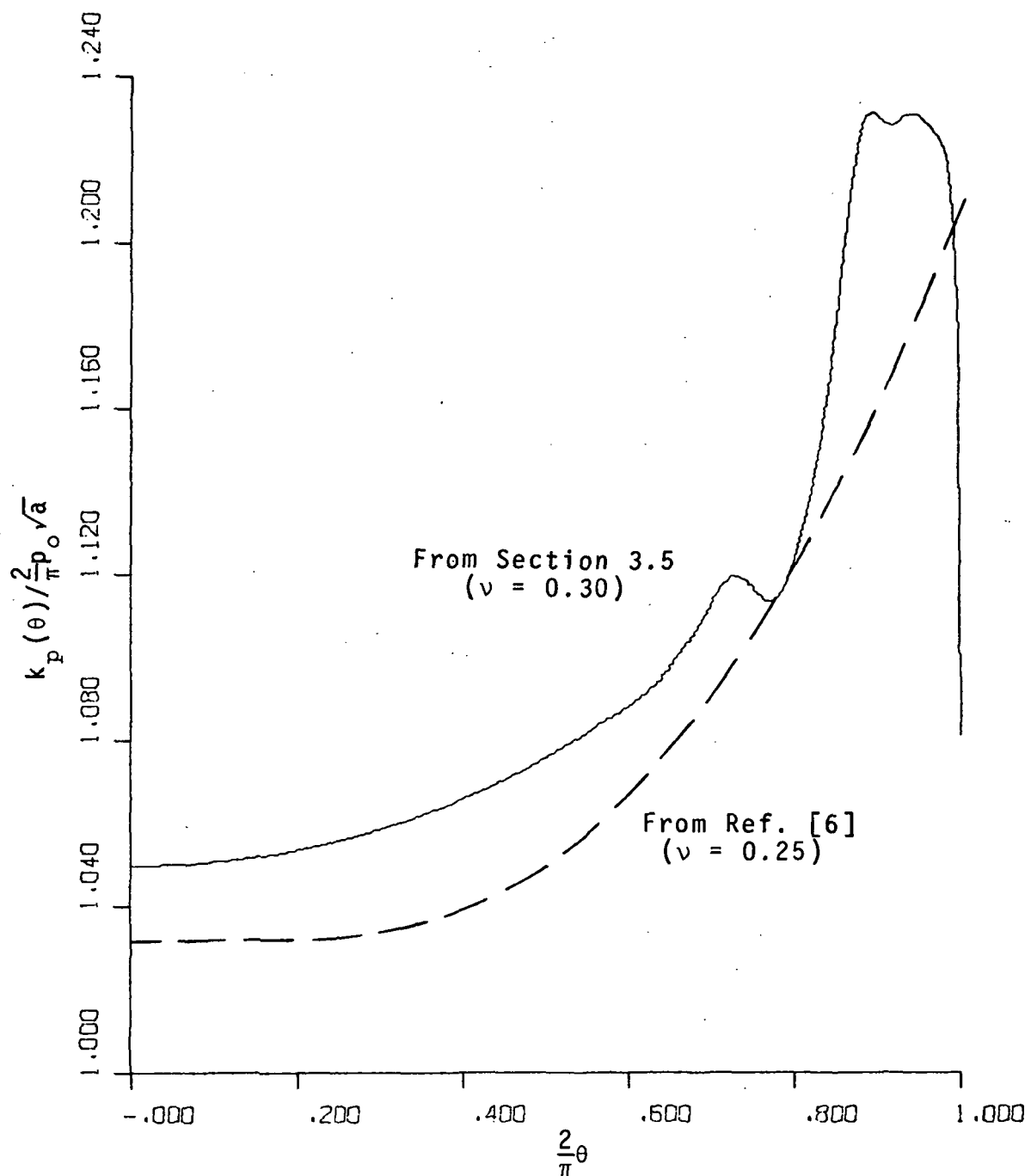


Fig. 3.8: Stress intensity factor for Fig. 3.6
 -94-

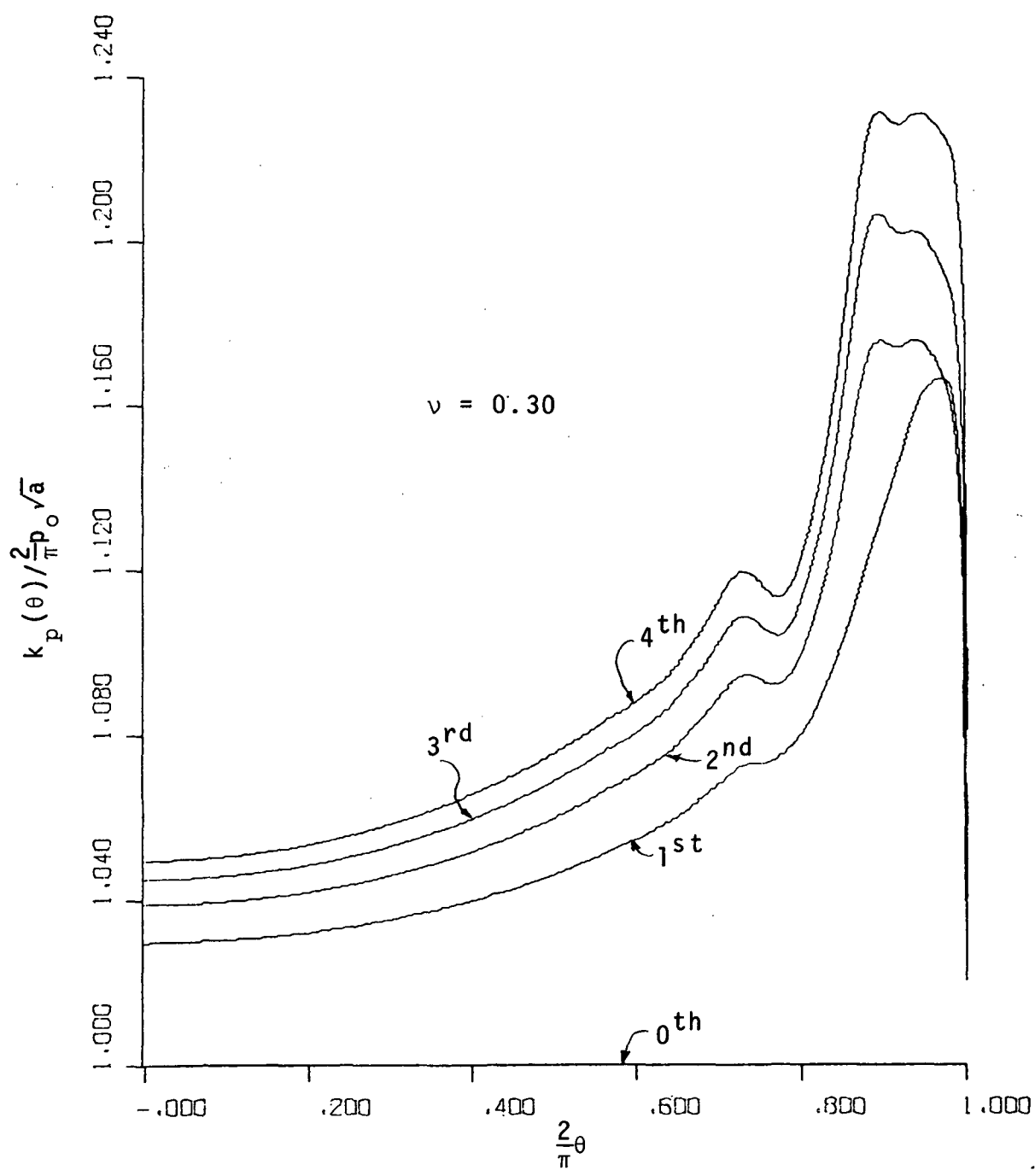


Fig. 3.9: Successive iterations for the stress intensity factor

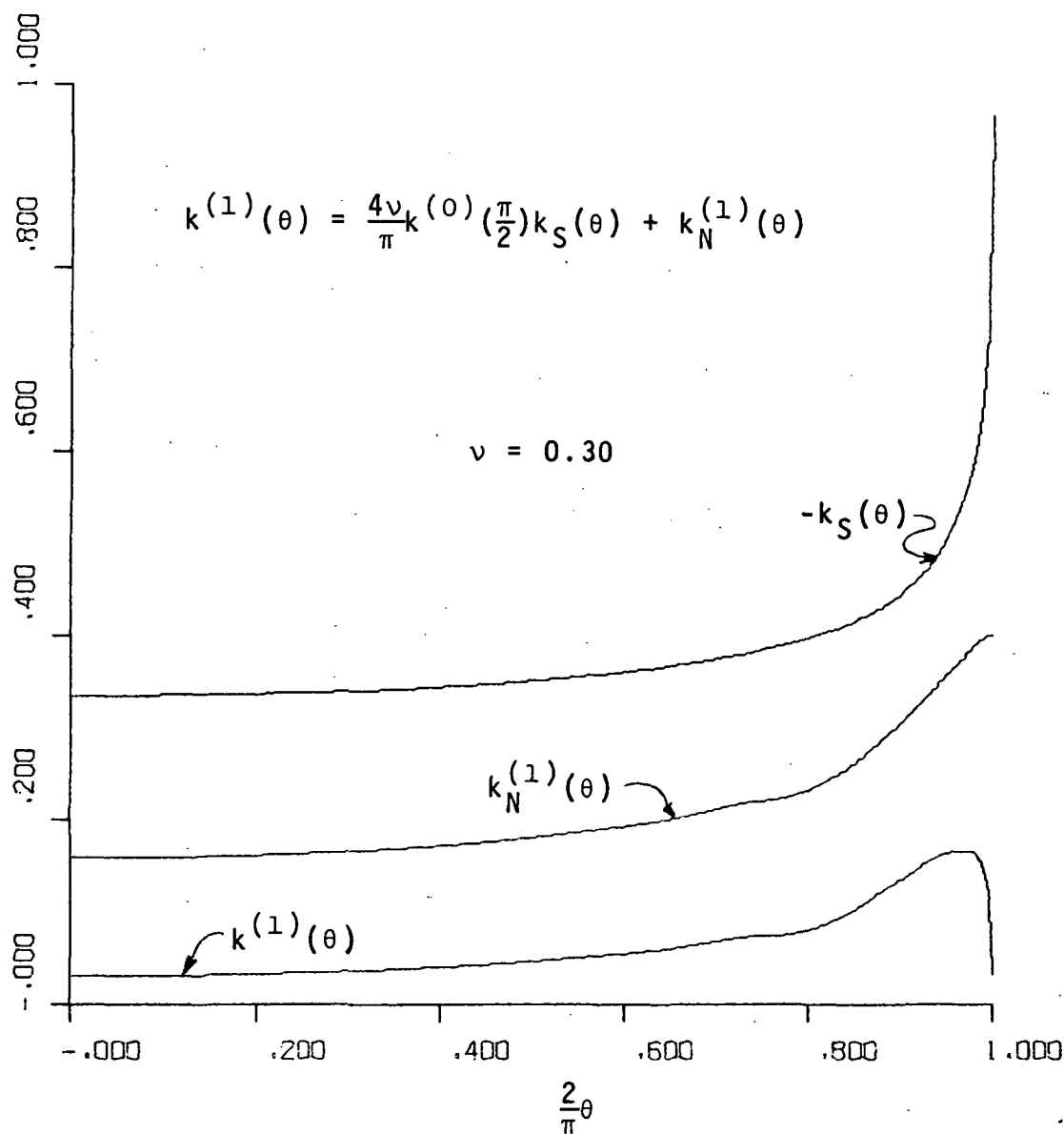


Fig. 3.10: Separate contributions to the stress intensity factor in first iteration

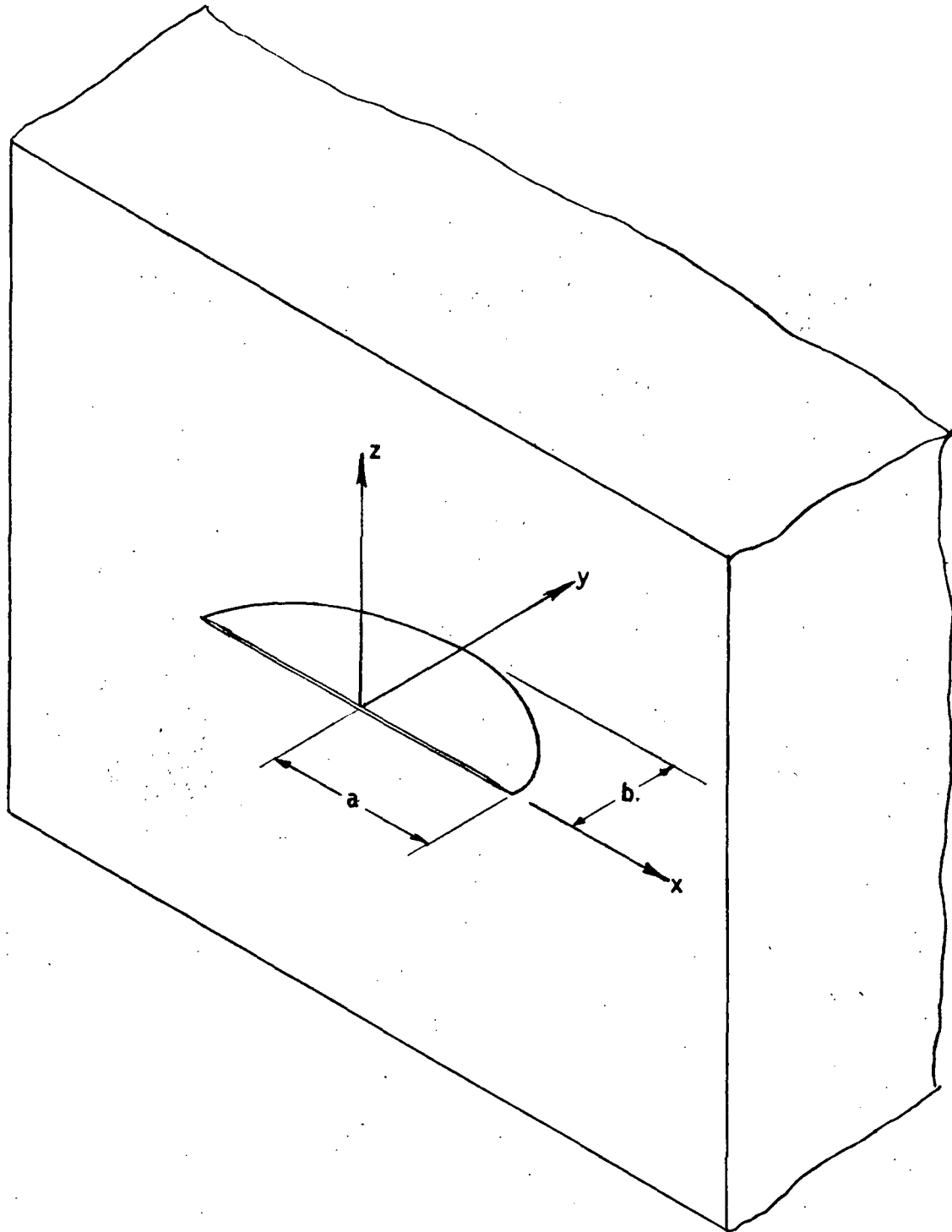


Fig. 4.1: Semi-elliptical surface crack

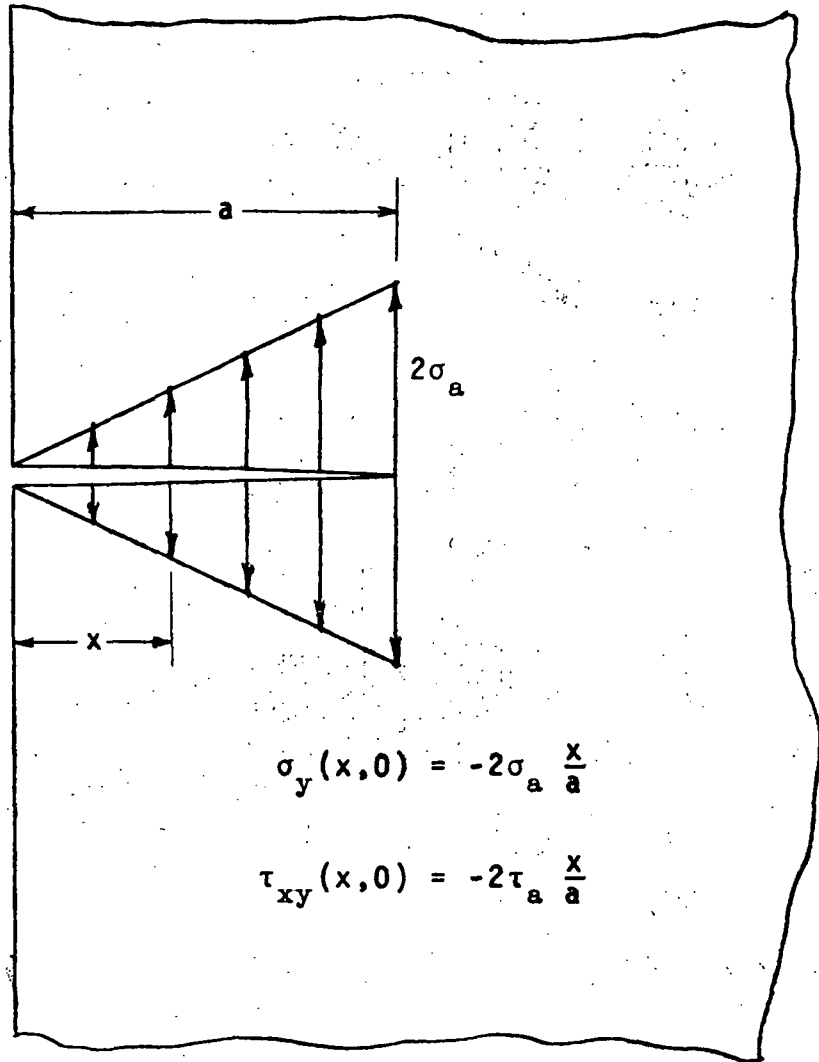


Fig. A-1: Linearly loaded edge crack

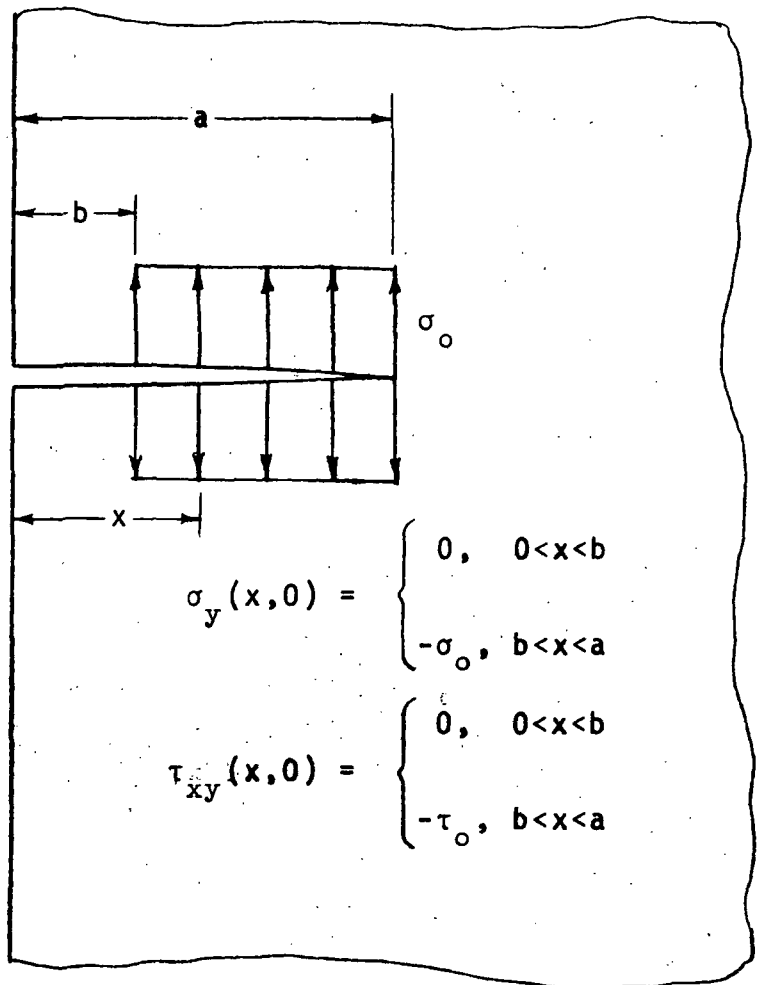


Fig. A-2: Partially loaded edge crack

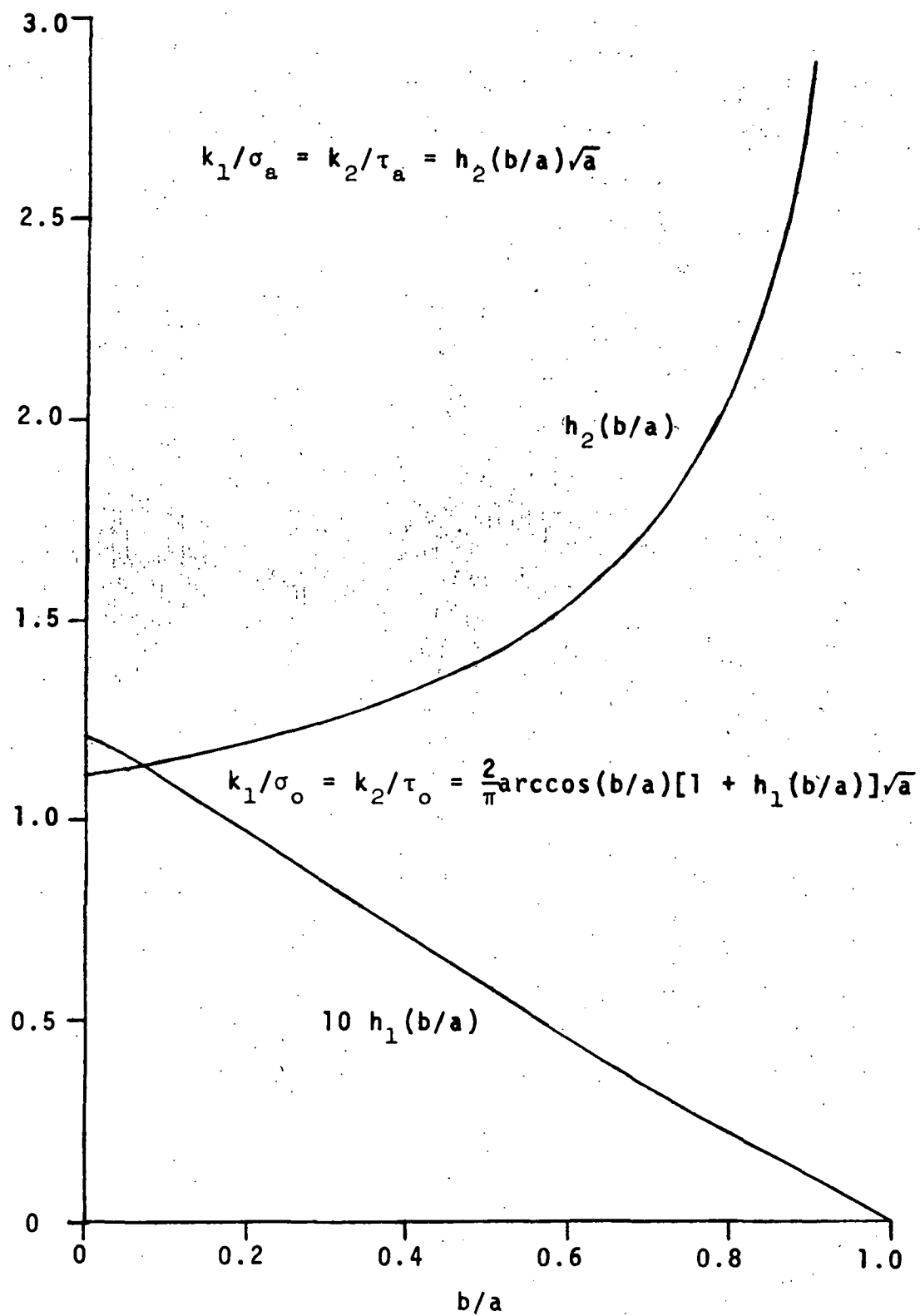


Fig. A-3: Correction factors for partially loaded edge crack
-100-

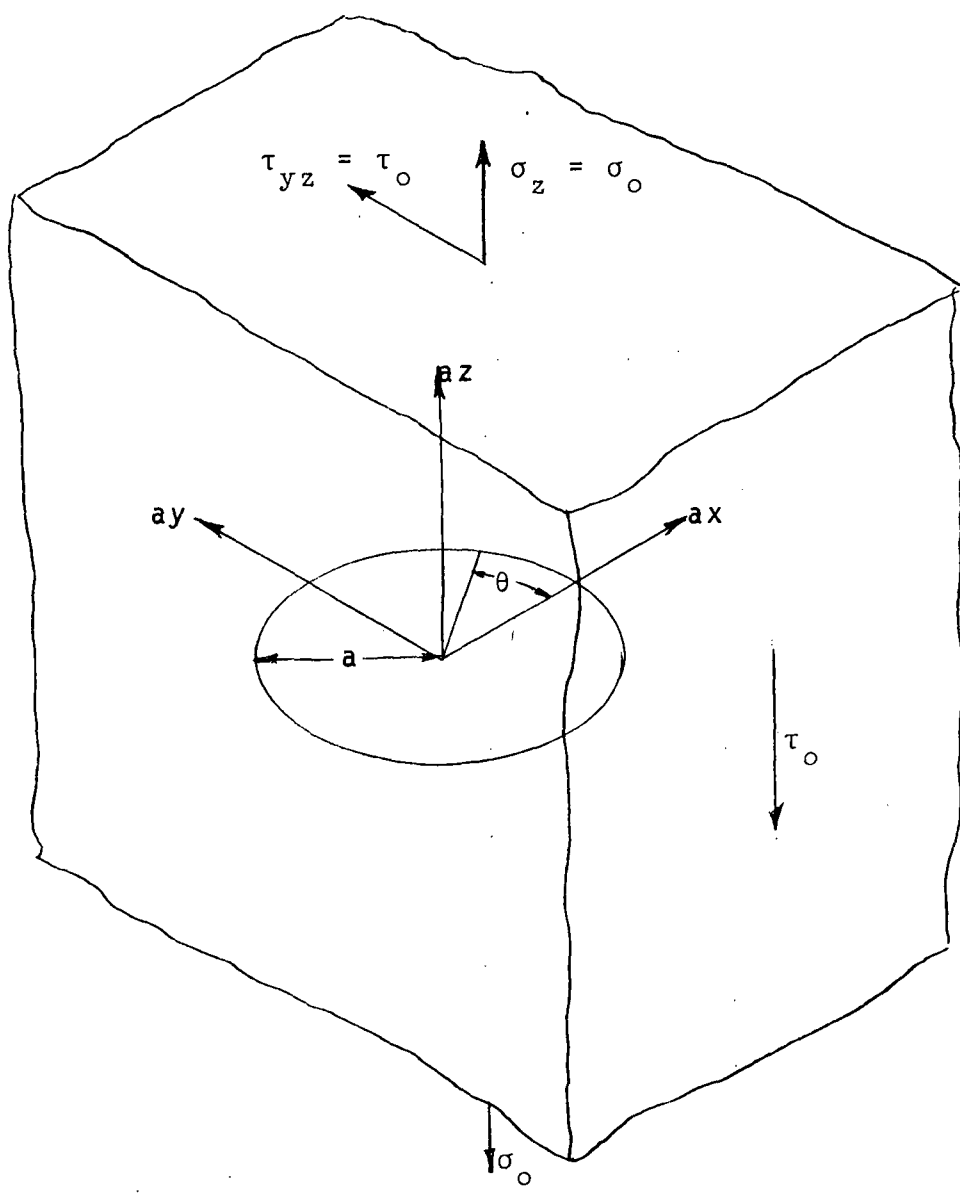


Fig. A-4: Penny-shaped crack in an infinite body under uniaxial tension and uniform shear

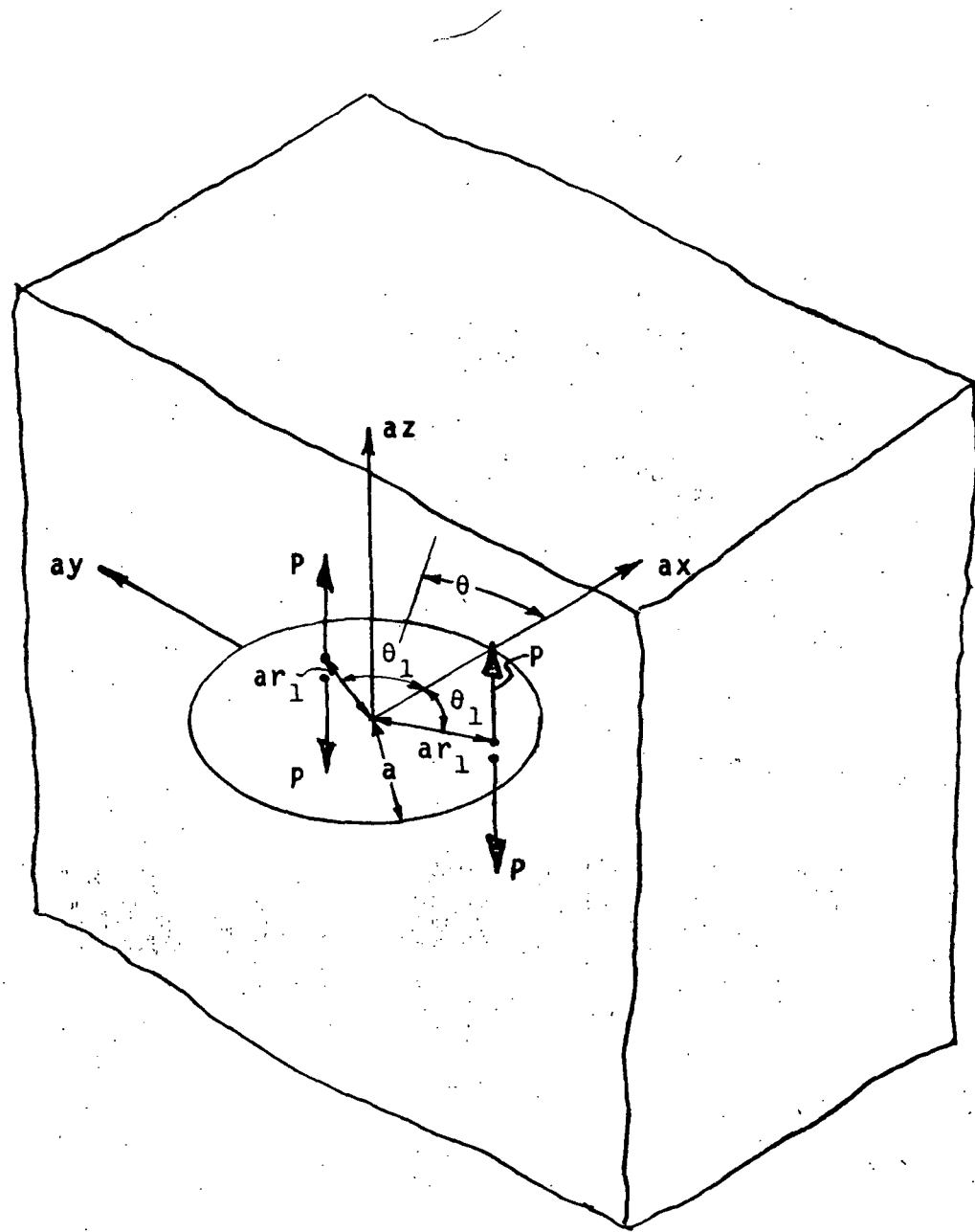


Fig. A-5: Concentrated forces on a penny-shaped crack

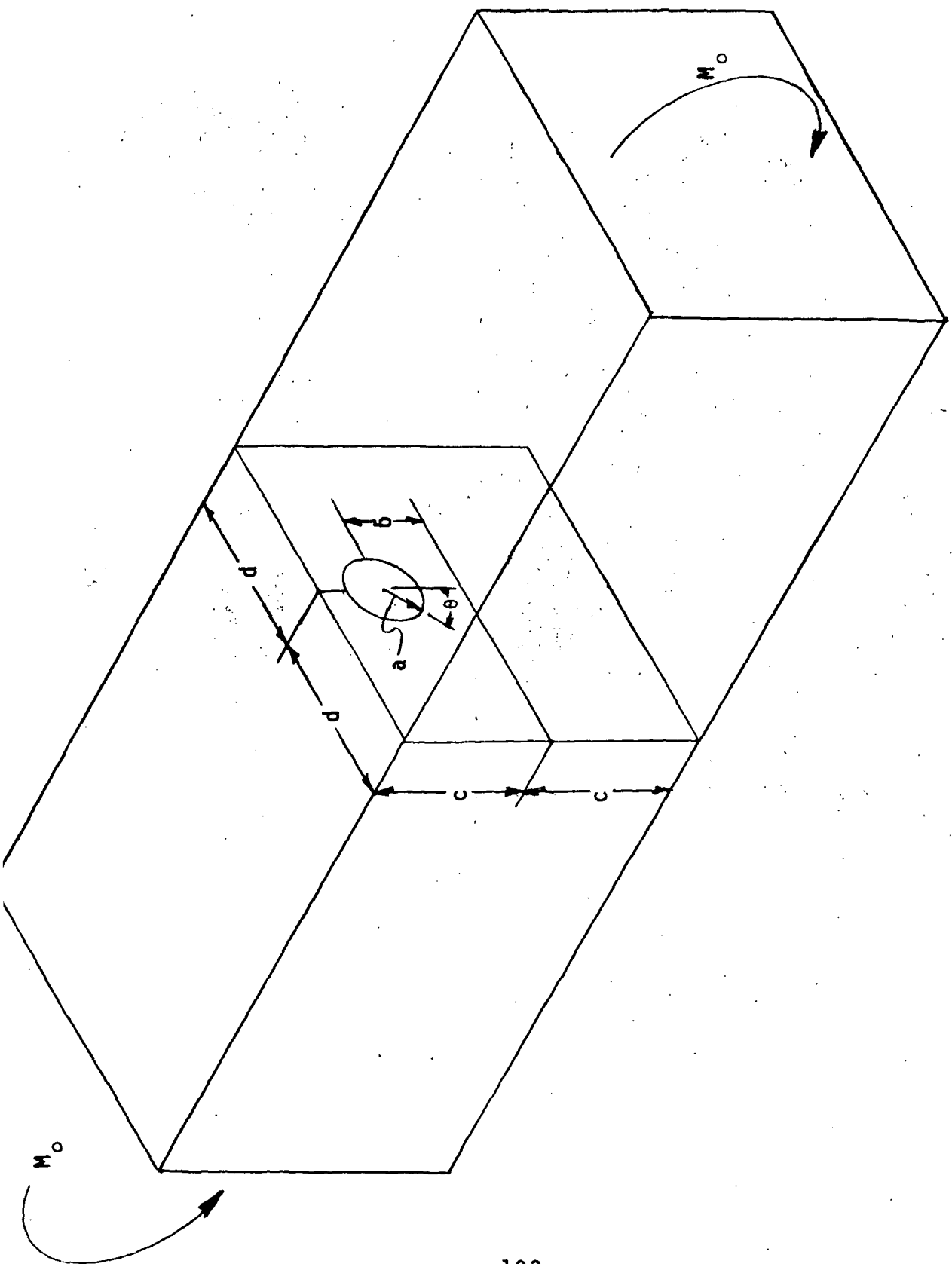


Fig. A-6: Penny-shaped crack in a cross-section of a beam under pure bending